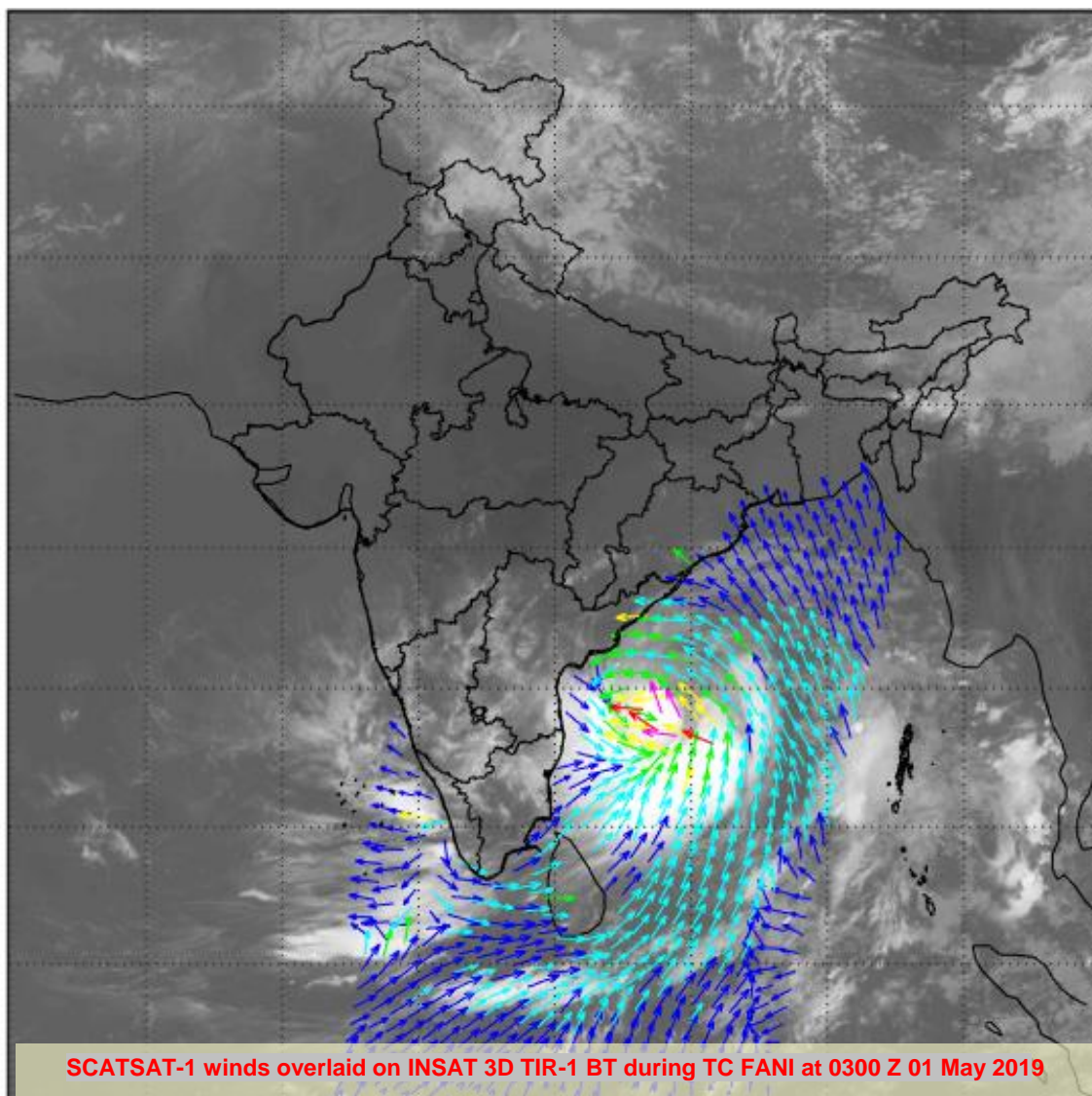




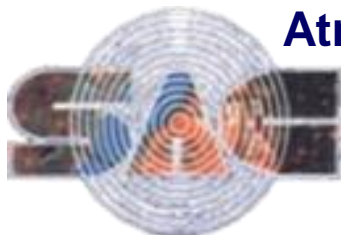
Real-time Monitoring and Prediction of Tropical Cyclone FANI

SAC/EPSA/AOSG/ASD/SR-15/2019



MAY 2019

Atmospheric and Oceanic Sciences Group
Space Applications Centre (ISRO)
Ahmedabad-380015



Document Control and DATA Sheet

Report No.	SAC/EPISA/AOSG/SR/15/2019
Date	May, 2019
Title	Real-time monitoring and prediction of tropical cyclone FANI
Type of Report	Scientific Report
No. of Pages	40
Authors	Neeru Jaiswal, C. M. Kishtawal, R. M. Gairola
Number of Figures	16
Number of Tables	7
Number of References	19
Originating Unit	AOSG/EPISA/SAC
Abstract	<p>The accurate and timely advance prediction of tropical cyclones is very important to disseminate the warnings and preparedness. Prediction of development of any cyclone system in the North Indian Ocean is being done at Space Applications Centre (ISRO) Ahmedabad, using the in-house developed algorithms. Once the low pressure system is formed, it is continuously monitored by satellite observations. The tropical cyclone track is predicted and updated. These forecasts and satellite based cyclone inputs are disseminated through web-portal SCORPIO linked to MOSDAC. The real-time prediction of cyclone FANI and its structural analysis using satellite observations are presented in this report. The surface wind observations over TC FANI by different satellites e.g. SCATSAT-1, CYGNSS, WINDSAT and SMAP are also presented.</p>
Key words	Tropical cyclone, track prediction, cyclogenesis, center determination, satellite observations
Security classification	Unrestricted

Acknowledgements

The authors are thankful to the Director, Space Applications Centre (ISRO), Ahmedabad and the Deputy Director of EPSA, SAC-ISRO. The authors acknowledge the Joint Typhoon Warning Centre (JTWC) and Regional Specialized Meteorological Centre (RSMC) for tropical cyclones over North Indian Ocean, India Meteorological Department (IMD), Delhi for providing real time cyclone track through their websites. IMD is also acknowledged for providing the best track estimates for TC FANI. The satellite observations of SCATSAT, INSAT-3D, INASAT-3DR and SAPHIR were obtained from MOSDAC (www.mosdac.gov.in). The satellite observations of WINDSAT and CYGNSS were obtained from PO-DAAC NASA website (<https://podaac.jpl.nasa.gov/>). SMAP products have been obtained from REMSS website (<ftp://ftp.remss.com/smap/wind/>).

Table of Contents

1. INTRODUCTION.....	5
1.1. OVERVIEW OF TROPICAL CYCLONE FANI (27 APRIL - 03 MAY 2019).....	5
2. DATA AND METHODOLOGY.....	8
2.1 TROPICAL CYCLOGENESIS PREDICTION	8
2.2 CYCLONE TRACK PREDICTION.....	8
2.2.1 SAC-Lagrangian Advection Model.....	8
3. RESULTS: PREDICTION OF TC FANI.....	10
3.1 CYCLOGENESIS PREDICTION OF TC FANI.....	10
3.2 REAL-TIME TRACK PREDICTION OF TC FANI.....	14
3.3 INTENSITY PREDICTION OF TC FANI.....	22
3.4 SHIP AVOIDANCE REGION PREDICTION FOR TC FANI.....	23
4. SATELLITE OBSERVATIONS OVER TC FANI.....	24
4.1 INSAT 3D	24
4.2 SAPHIR	26
4.3 SATELLITE BASED SURFACE WIND OBSERVATIONS OVER TC FANI	27
4.3.1 SCATSAT-1.....	27
4.3.2 CYGNSS.....	29
4.3.3 SMAP.....	31
4.3.4 WINDSAT	34
4.3.5 Comparison of Satellite Wind Speed Products	36
5. CONCLUSIONS	37
REFERENCES	39

1. Introduction

Indian sub-continent is one of the most adversely affected cyclone active basins that experience on an average 4-5 cyclones every year. In comparison to other cyclone basins this region is the most vulnerable due to relatively dense coastal population, shallow bottom topography and coastal configuration. Though the cyclones formed in this region are considered to be weaker in intensity and smaller in size as compared to other regions, yet the number of deaths in the region is highest in the globe. To overcome such loss, advance prediction of cyclones in terms of their genesis, track and intensity is highly important. The timely prediction of impending cyclonic activity can save life of people and help in decision making for taking preventive measures like evacuation during the cyclone landfall. The predictions of TC are generated based on the models using satellite observations and ground based radar networks when cyclone reaches close to the land. Due to the advancements in numerical prediction models, computational resources and satellite observations with high temporal and spatial resolutions, during the last decades, the track prediction accuracy has improved drastically. However, the prediction of cyclogenesis and cyclone intensity is still challenging.

Prediction of development of any cyclone system in the North Indian Ocean (NIO) including the Bay of Bengal (BoB) and Arabian Sea is being done as a regular exercise at Space Applications Centre (ISRO) Ahmedabad, using the in-house developed algorithms. Once the system is developed in the NIO basin its track and intensity are predicted in real-time and disseminated through web-portal Satellite based cyclone real-time prediction in Indian Ocean (SCORPIO) linked to MOSDAC (www.mosdac.gov.in). The similar exercise was performed during the formation of cyclone “FANI” in NIO during 27 April -03 May 2019, which has been discussed in the present report.

1.1. Overview of Tropical cyclone FANI (27 April - 03 May 2019)

The tropical cyclone “FANI”, was classified by IMD as extremely severe cyclonic storm. It was originated from a tropical depression formed at west of Sumatra in the North Indian Ocean on 26 April 2019. Vertical wind shear at first hindered the storm's development, but conditions became more favorable on 30 April. TC FANI rapidly intensified into an extremely severe cyclonic storm and reached its peak intensity on 2

May, as a high-end extremely severe cyclonic storm, and the equivalent of a high-end Category 4 major hurricane on Saffir simpson scale. FANI made landfall as extremely severe cyclone category on the 3rd May morning hours and its convective structure rapidly degraded thereafter, dissipating on 5 May. Prior to its landfall, authorities in India and Bangladesh moved at least a million people each from FANI's predicted path onto higher ground and into cyclone shelters, which is thought to have reduced the resultant death toll. The Observed track of TC FANI with its intensity categories provided by JTWC has been shown in the Figure 1. The IMD classification of cyclone categories is given in Table 1.

JTWC Observed track of Cyclone FANI (26 April -03 May 2019)

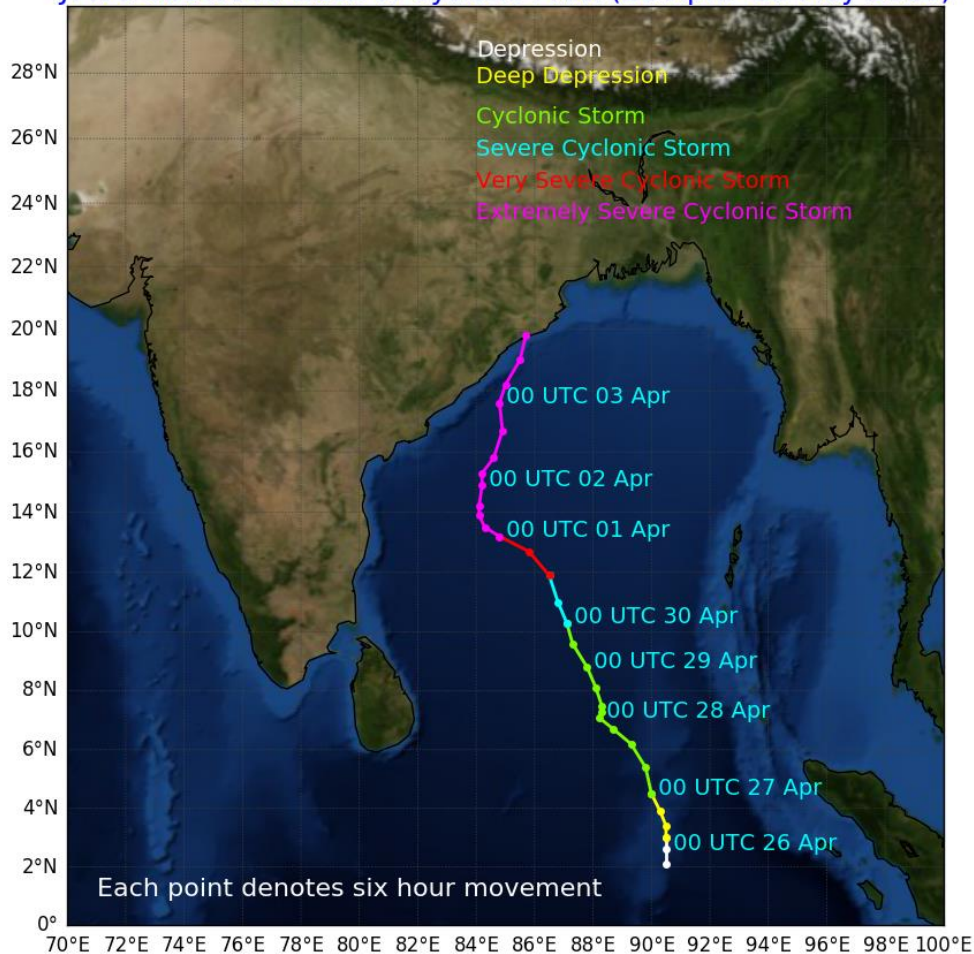


Figure 1: Real-time observed track (JTWC) of cyclone FANI with its intensity categories.

Table 1: IMD classification of categories of cyclonic system

System	Associated wind speed (knots)
Low pressure area	<17
Depression	17-27
Deep Depression	28-33
Cyclonic Storm	34-47
Severe Cyclonic Storm (SCS)	48-63
Very SCS (VSCS)	64-85
Extremely SCS (ESCS)	86-119
Super Cyclonic Storm(SuC)	>119

The cyclone name “FANI”, was given by Bangladesh. As per global convention, the eight countries that make up the Indian Ocean Region—India, Bangladesh, Sri Lanka, Thailand Pakistan, Maldives, Myanmar, Oman—have drawn up a list of names for tropical cyclones, which are assigned serially with the alphabetic order of the nation’s name.

Development stages of the cyclone FANI were continuously monitored by the visible and infrared observations from geo-stationary satellites viz., INSAT-3D and high resolution microwave satellite viz., SAPHIR onboard Megha-Tropiques. SCATSAT provided very good observations over these cyclonic systems, which were found to be very helpful for its prediction and structural analysis. The surface wind observations provided by advanced satellites like CYGNSS, SMAP and WINDSAT have also been discussed in this report. Using the observations and models, the real-time predictions of cyclone track, intensity, rainfall and wind structure were performed at SAC-ISRO. The real-time prediction of the cyclone using in-house developed algorithms and the satellite observations over the system that helped in monitoring and prediction has been discussed in this report. The in-house developed techniques used for the cyclone prediction are briefly discussed in the section 2. The separate sections are made for the detail discussion of satellite estimated surface wind analysis and its comparison w.r.t IMD and JTWC estimates.

2. Data and Methodology

A system has been formed in the SAC to predict the cyclones from its birth till death. This starts with predicting the earliest signatures of development of a low pressure system i.e. tropical cyclogenesis. After the declaration of system as tropical cyclone or cyclonic storm by JTWC or IMD, its track is predicted and updated during the life period of the cyclone till its landfall occurs. The track prediction also includes its landfall time and position prediction. Predictions of cyclone intensity is also generated using NWP models. All these predictions are disseminated in the real-time through a web server “Satellite based cyclone observations and real-time prediction in Indian Ocean” i.e. SCORPIO linked with MOSDAC (www.mosdac.gov.in).

2.1 Tropical Cyclogenesis Prediction

A cyclone genesis parameter, termed the genesis potential parameter (GPP), for the Indian Sea was proposed by Kotal et al. 2019. The parameter is defined as the product of four variables, namely vorticity at 850 hPa, middle tropospheric relative humidity, middle tropospheric instability, and the inverse of vertical wind shear. The variables are calculated using the National Centers for Environmental Prediction (NCEP), USA, reanalysis data, averaged within a circle of 2.5° radius around the centre of cyclonic system. The GPP, at early development stage of a cyclonic storm provides a useful predictive signal for intensification of the system. This parameter has been computed in this work based on NCEP-GFS analysis data during 00 UTC 20 April-27 April 2019 to investigate the cyclogenesis signatures of TC FANI.

2.2 Cyclone Track Prediction

After the formation of tropical cyclone in the North Indian Ocean, track predictions are carried out using in-house developed Lagrangian advection cyclone track prediction model (SAC-LAGAM). A brief summary of the model has been given in the following subsections.

2.2.1 SAC-Lagrangian Advection Model

SAC-Lagrangian Advection model is dynamical framework based computationally efficient model (Singh et al, 2011; 2012). It requires the high resolution $0.5^0 \times 0.5^0$

atmospheric winds and temperature forecasts from Global forecast System (GFS), which is global numerical weather prediction model run by NOAA, and the initial position of cyclone which is obtained from JTWC. The cyclone track prediction is provided using SAC- Lagrangian Advection model up to 96 hour with 6 hour interval. As a first step, the steering flow has been computed for every 6-hour forecast interval up to 96 hours, using the analysis as well as forecast wind fields data at 21 pressure levels (100-1000 mb) by the weighted average scheme. The weight for each level was assigned by estimating the potential vorticity (PV) which is adapted from the study by Hoover et al., 2006. Then a cyclonic vortex is removed using a synthetic cyclone which is constructed by using the vorticity equation (Chan and Williams, 1987):

$$\frac{\partial \zeta}{\partial t} + \mathbf{v} \cdot \nabla (\zeta + f) = 0$$

Where ζ is the vorticity and $f = \beta y + f_0$. Here y denotes latitudinal displacement, f_0 is the value of coriolis parameter at $y = 0$ and β is the rate of change of coriolis parameter with latitude. In case of axisymmetric vortex, the velocity is calculated using the equation (Chan and Williams, 1987):

$$v(r) = V_m \left(\frac{r}{r_m} \right) \exp \left[\frac{1}{b} \left(1 - \left(\frac{r}{r_m} \right)^b \right) \right]$$

Where V_m and r_m denote the maximum value of tangential velocity and the radius at which V_m occurs, respectively. This synthetic cyclone was used to remove the existing cyclonic wind fields present in the steering flow to achieve the residual steering current. To avoid the discontinuity of wind fields due to removal of cyclonic circulation, tapered weights $W(k)$ are used for generation of residual flow fields. Now, resulting steering flow that is obtained after removing the cyclonic vortex from steering flow is used in model to forecast the cyclone track. The computation for the trajectory of the cyclone (or the cyclone track) is initiated by interpolating the steering wind from model grid points to the initial location of the cyclone (Brand, 1981).

The above discussed techniques and models, which are used in the real-time for the prediction of cyclone FANI.

3. Results: Prediction of TC FANI

Real-time cyclogenesis and track prediction of TC FANI was carried out at SAC using the above discussed algorithms. The results of real-time prediction and the validation of the forecasts have been discussed in this section.

3.1 Cyclogenesis prediction of TC FANI

The genesis potential parameter (GPP) was computed based on the product of four variables, namely: vorticity at 850 hPa, middle tropospheric relative humidity, middle tropospheric instability and the inverse of vertical wind shear at all grid points using GFS 0.5 degree analysis data. Higher value of the GPP over a region indicates higher potential of genesis over the region. Region with GPP value equal or greater than 30 is found to be high potential zone for cyclogenesis. The threshold for distinguishing developing and non-developing systems is 8.0 (Kotal et al., 2009). The values of GPP with all the governing variables during 00 UTC 21 -27 April 2019 have been shown in Figure 2 a-g. The earliest signature of developing system was found on 23 April 2019 as GPP value was 13.6 which was exceeding the threshold value. This has to be noticed that the vortex was very close to the equator at that time (-0.5° latitude). On 00 UTC 25th April the vortex moved at 2.5 degree Latitude and GPP was increased as 16.21 which was strongly indicating the development of tropical cyclone in Bay of Bengal region.

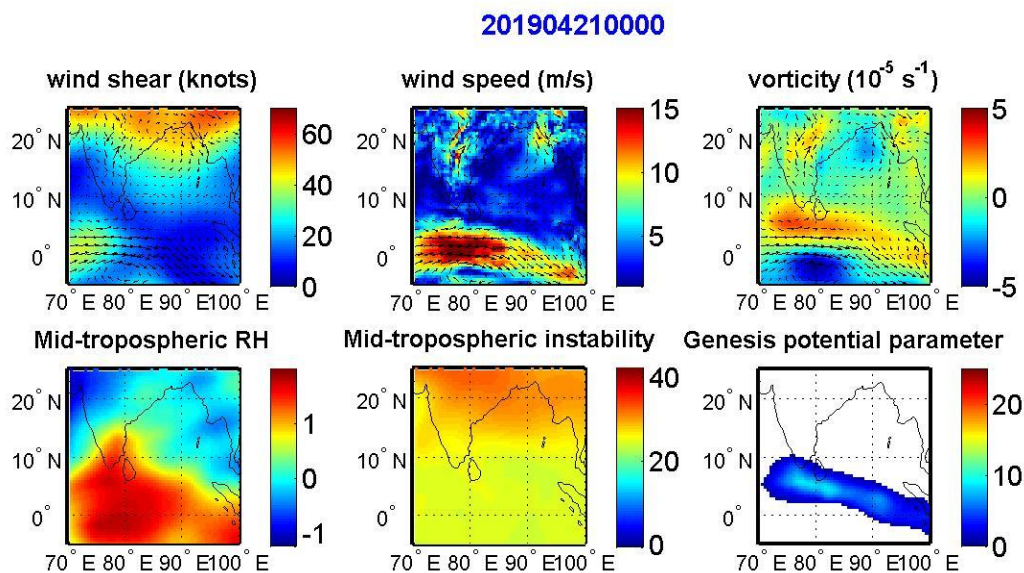


Figure 2a: Vertical wind shear, 850-hpa wind speed, 850-hpa vorticity, mid tropospheric relative humidity, instability and the GPP parameter at 00 UTC 21 April 2019.

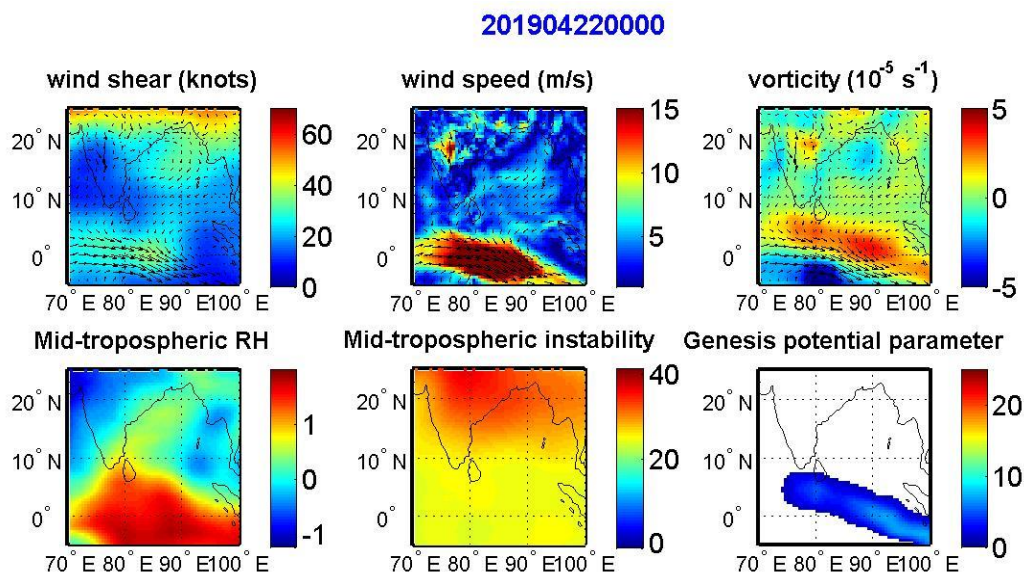


Figure 2b: Vertical wind shear, 850-hpa wind speed, 850-hpa vorticity, mid tropospheric relative humidity, instability and the GPP parameter at 00 UTC 22 April 2019.

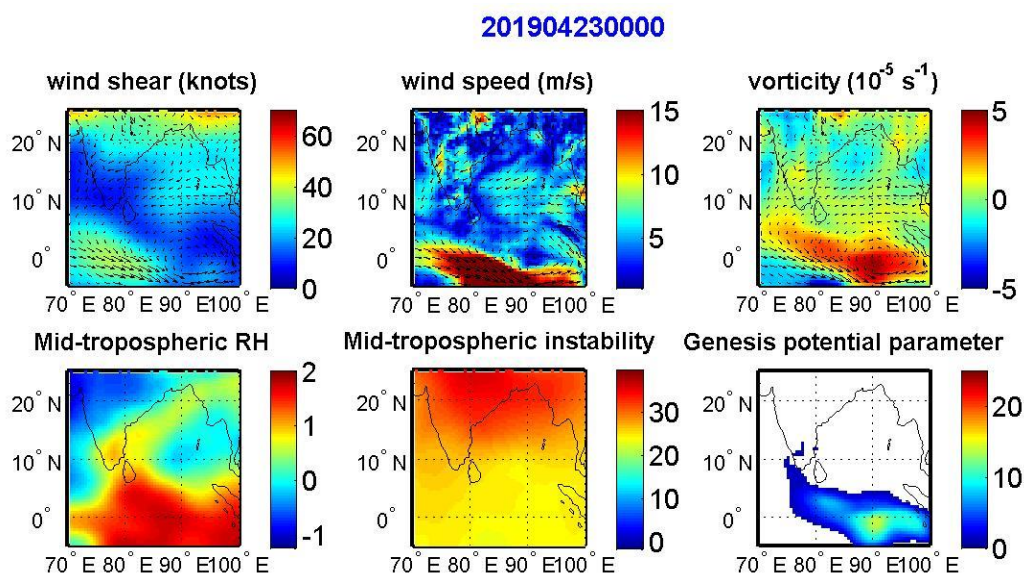


Figure 2c: Vertical wind shear, 850-hpa wind speed, 850-hpa vorticity, mid tropospheric relative humidity, instability and the GPP parameter at 00 UTC 23 April 2019.

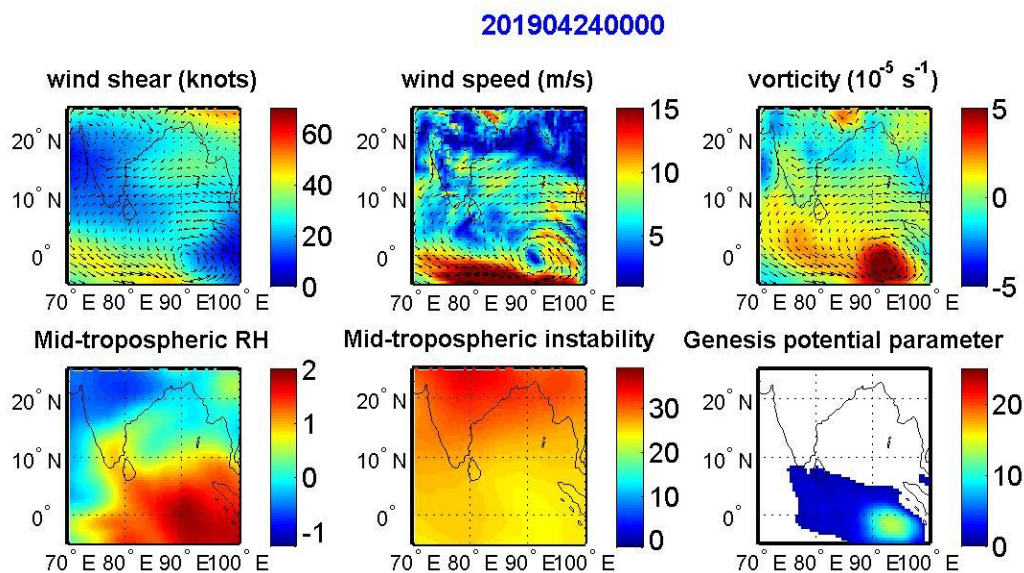


Figure 2d: Vertical wind shear, 850-hpa wind speed, 850-hpa vorticity, mid tropospheric relative humidity, instability and the GPP parameter at 00 UTC 24 April 2019.

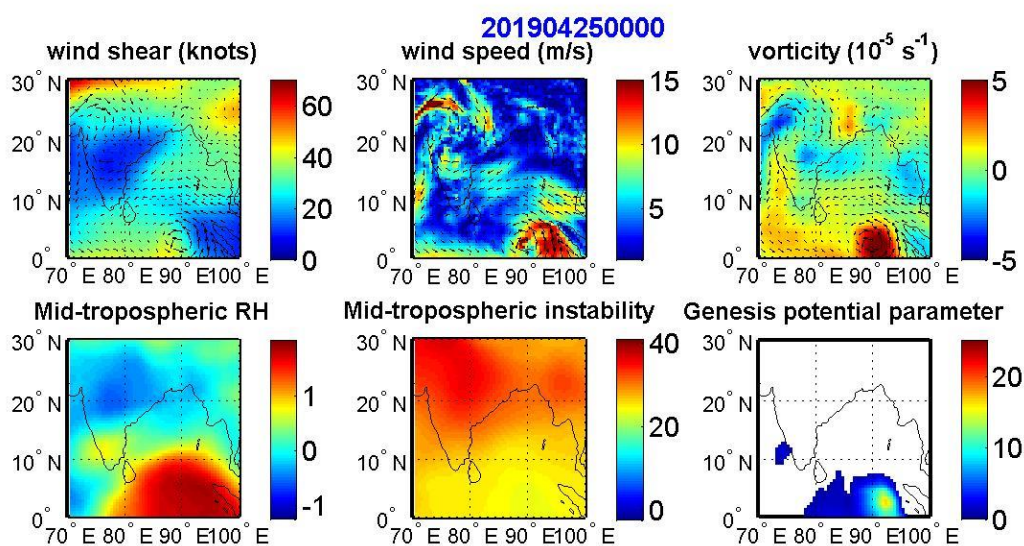


Figure 2e: Vertical wind shear, 850-hpa wind speed, 850-hpa vorticity, mid tropospheric relative humidity, instability and the GPP parameter at 00 UTC 25 April 2019.

201904260000

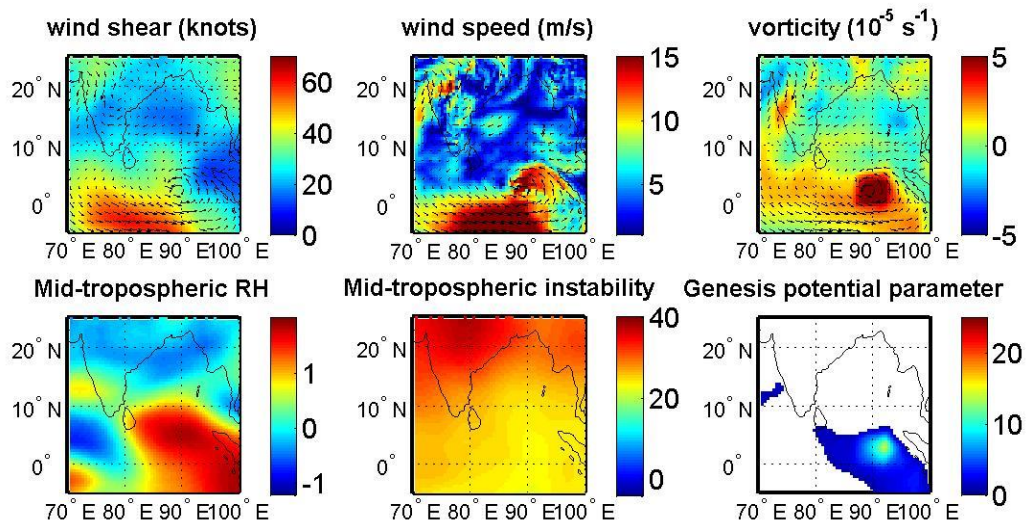


Figure 2f: Vertical wind shear, 850-hpa wind speed, 850-hpa vorticity, mid tropospheric relative humidity, instability and the GPP parameter at 00 UTC 26 April 2019.

201904270000

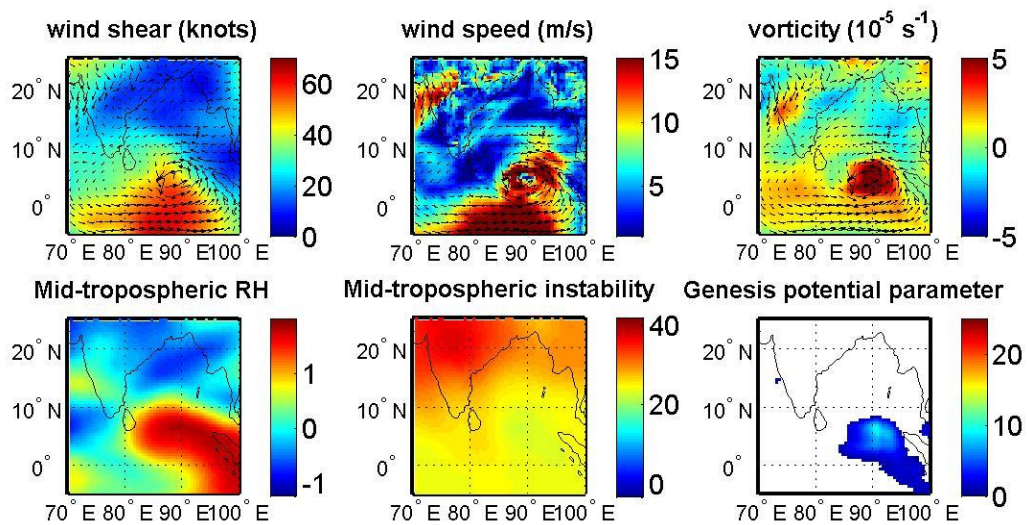


Figure 2g: Vertical wind shear, 850-hpa wind speed, 850-hpa vorticity, mid tropospheric relative humidity, instability and the GPP parameter at 00 UTC 27 April 2019.

3.2 Real-time track prediction of TC FANI

After formation of TC FANI its track was predicted using the SAC-Lagrangian Advection model. The cyclone track forecast using SAC-Lagrangian model was generated on 00, 06, 12 and 18 UTC of 27th April -02nd May 2019 and have been shown in the Fig. 3. The initial position of cyclone in the forecasts was taken from the real-time provided cyclone bulletins of JTWC. Each point in the figure is representing the six hours' movement of the cyclone. Each day forecasts have been presented in different colors with four different marker styles for four initial forecasts hours in a day. IMD best track and JTWC real-time observed track has also been presented in the figure.

In the real-time only 00 UTC track were disseminated over the website which have been provided in Fig. 4. Based on the past track error statistics of the model, the cone of uncertainty has been computed and shown as a shaded region along the predicted track.

It can be seen from the figure that the tracks generated after 06 UTC 29 April are showing the system making landfall over the east coast of India in the Odhisa state. The forecasted track were compared with JTWC observed track and the error of track forecast has been estimated. The direct position error (DPE), cross track (CT) and along track (AT) component of track forecast error were calculated with respect to JTWC observed track position values for all the forecasts generated on different initial conditions and have been given in the Table 2, 3, and 4, respectively. The schematic showing the computation of the track errors is shown in the Fig. 5.

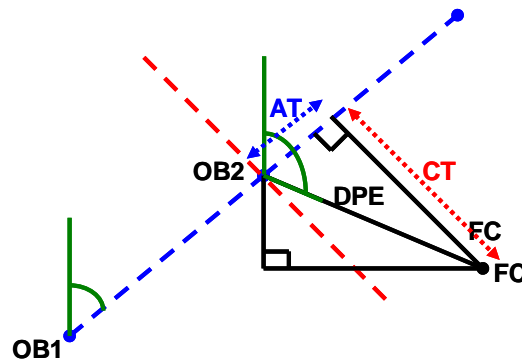


Figure 5: Schematic showing the positional forecast errors (Heming, 1994).

The position error of track forecast by SAC-model is also estimated w.r.t. IMD best track positions. The values have been summarized in the Table 5.

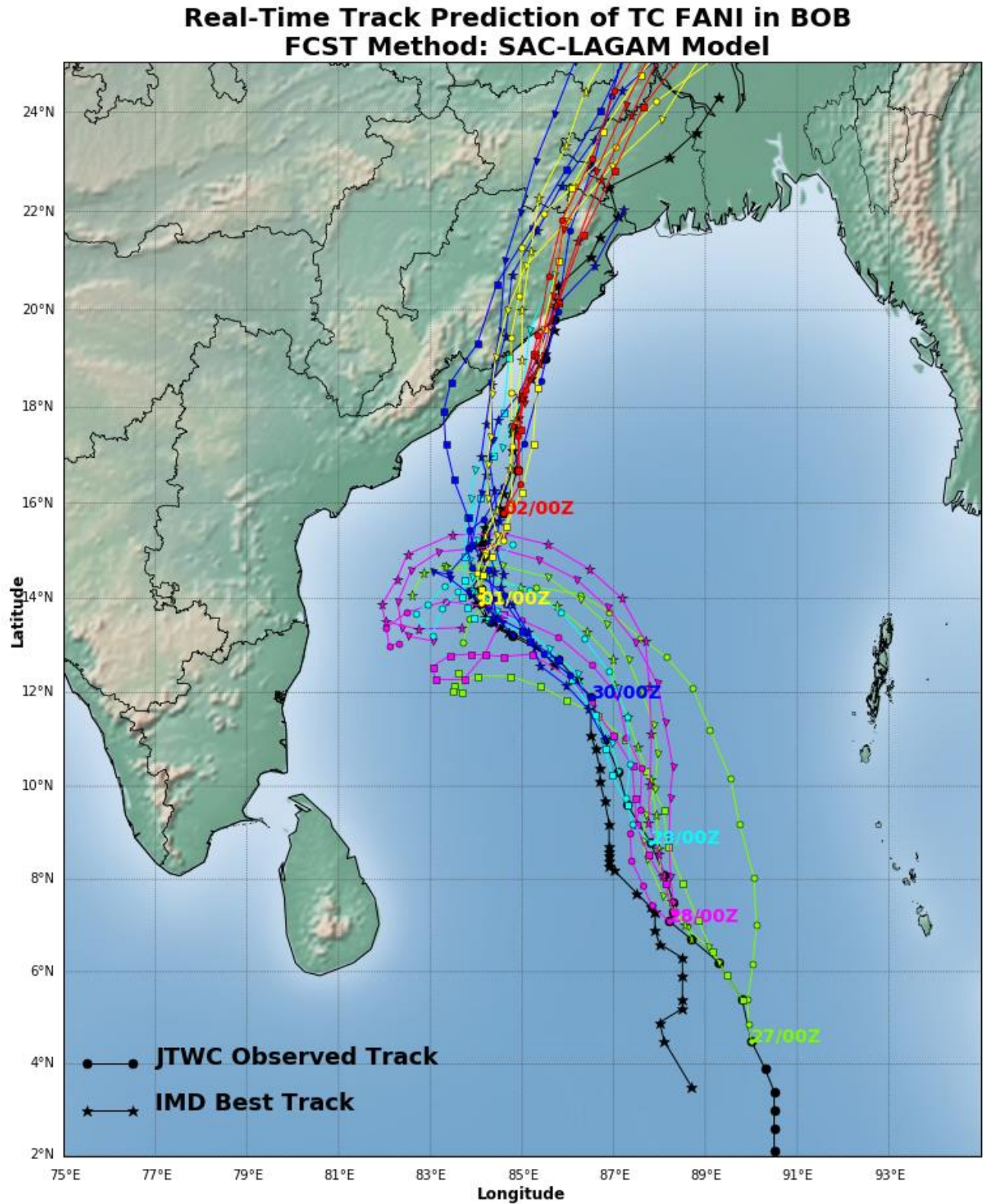


Figure 3: Real-time predicted track of TC FANI at 00,06,12,18 UTC 27 April-02 May 2019 with the JTWC observed track.

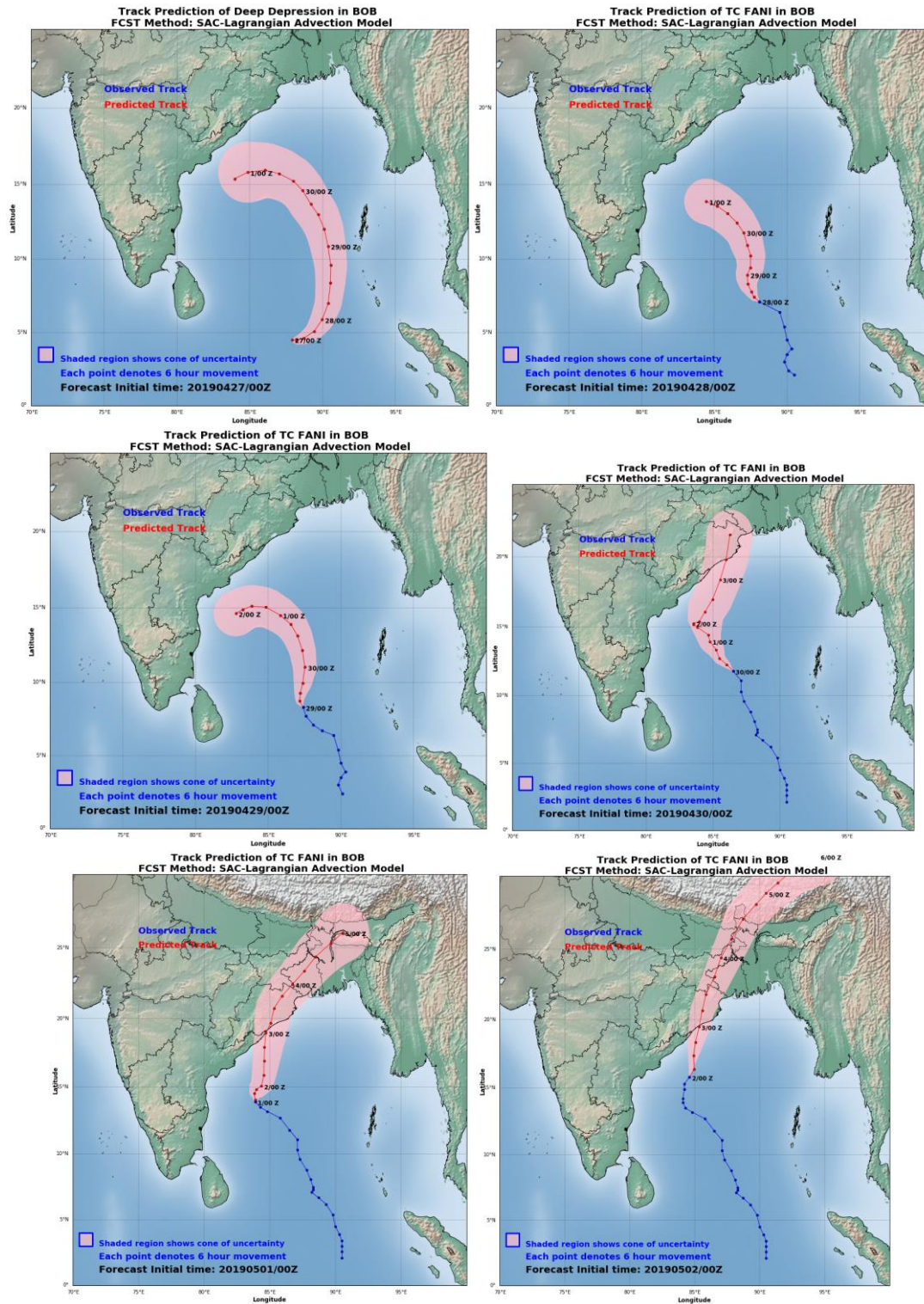


Figure 4: Real-time predicted track of TC FANI at 00 UTC 27 April-02 May, 2019.

Table 2: Direct position error of SAC-Lagrangian advection track prediction model for TC FANI w.r.t JTWC real-time observed track

FCST Initial time	Track Error (km) in different Forecast Lead time															
	6	12	18	24	30	36	42	48	54	60	66	72	78	84	90	96
2700	62.01	111.45	159.78	210.91	210.68	246.63	278.94	302.46	318.84	296.49	254.03	206.97	161.65	128.09	67.75	44.93
2706	35.42	56.95	69.59	73.44	136.20	154.58	170.56	158.08	144.66	131.59	124.70	121.47	126.01	173.80	217.46	247.53
2712	43.03	47.19	46.45	121.55	95.30	65.42	76.40	103.55	121.71	121.48	163.80	222.61	219.11	167.86	73.64	42.87
2718	39.63	26.16	69.11	63.89	66.05	80.46	76.47	76.30	61.55	129.08	174.61	162.21	99.17	33.66	96.68	169.36
2800	53.81	83.02	84.95	53.21	32.29	56.68	52.58	63.35	79.07	108.28	75.75	18.95	87.94	226.84	315.79	412.45
2806	50.17	62.26	54.26	23.45	36.81	23.02	12.28	52.68	61.31	87.43	122.43	173.17	289.79	355.84	402.50	438.14
2812	16.38	45.72	103.12	130.96	149.01	160.58	185.64	232.83	226.71	169.10	102.55	109.94	190.65	324.55	458.34	547.36
2818	35.67	66.54	81.69	112.11	141.35	209.40	271.51	264.18	208.26	139.74	91.47	187.07	294.03	447.78	543.57	591.00
2900	46.09	64.99	84.95	97.88	121.52	169.03	169.29	117.47	28.13	117.79	208.12	314.20	435.48	455.36	475.17	519.24
2906	17.33	20.04	42.05	53.62	88.64	80.60	39.10	70.27	129.37	149.83	179.49	237.40	235.11	250.68	251.48	240.90
2912	18.13	25.67	54.75	91.06	72.58	40.80	26.70	89.72	99.86	136.08	189.13	193.94	198.46	226.91	193.16	
2918	29.42	63.88	95.59	91.72	73.44	46.47	61.14	34.75	20.76	73.21	88.99	76.64	102.50	98.49		
3000	43.47	84.93	88.59	59.41	56.86	41.77	49.05	89.29	140.06	139.68	104.66	52.02	21.69			
3006	39.20	75.94	48.06	39.57	30.50	35.30	84.07	149.78	160.47	183.44	222.07	182.94				
3012	29.28	23.25	30.78	99.44	147.83	193.49	210.99	169.65	117.21	137.54	125.94					
3018	45.15	33.41	42.53	9.88	30.10	72.42	101.36	103.57	135.62	116.92						
0100	16.71	45.47	34.54	65.64	76.87	46.70	26.71	91.82	95.66							
0106	42.92	47.38	30.50	52.04	60.07	41.07	70.18	133.76								
0112	27.02	50.09	71.15	57.92	71.46	112.57	108.72									
0118	17.38	18.24	11.90	86.73	122.93	163.43										
0200	33.97	24.13	17.84	57.02	98.65											
0206	18.86	7.00	29.50	42.45												
0212	12.31	20.46	55.64													
0218	15.31	33.62														
Mean Error	32.86	47.41	61.19	77	91.39	102.02	109.04	127.97	126.43	139.86	148.52	161.39	189.35	240.82	281.41	325.38

Table 3: Cross track error of SAC-Lagrangian advection track prediction model for TC FANI w.r.t JTWC real-time observed track

FCST Initial time	Track Error (km) in different Forecast Lead time															
	6	12	18	24	30	36	42	48	54	60	66	72	78	84	90	96
2700	61.98	110.81	152.08	169.41	159.9	246.63	165.62	187.7	150.79	230.22	184.65	177.72	80.84	0.99	5.69	20.68
2706	35.42	55.95	52.21	72.54	136.2	147.33	161.18	138.02	144.17	122.46	63.34	47.29	35.4	2.46	153.77	247.53
2712	41.77	44.85	23.31	121.55	92.18	63.64	2.33	15.21	14.92	25.81	107.86	184.92	156.6	16.94	73.64	29.69
2718	35.69	20.38	69.11	63.61	53.55	20.37	45.69	26.89	7.25	85	151.04	116.54	8.24	33.66	36.72	169.36
2800	10.36	83.02	56.12	39.32	24.67	5.86	16.63	14.8	60.46	97.8	63.23	14.55	87.94	154.6	315.79	411.88
2806	50.17	58.48	52.16	3.74	6.78	0.86	11.25	52.14	58.85	70.1	96.37	173.17	275.39	355.84	365.44	433.8
2812	10.11	10.68	41.03	22.09	18.22	16.52	89.13	170.11	124.16	28.75	102.55	6.99	190.65	317.22	433.69	454.66
2818	34.76	63.39	50.33	31.82	21.34	103.2	190.52	138.54	50.28	139.74	36.18	187.07	275.37	396.28	413.06	587.14
2900	44.16	64.98	77.97	70.92	98.44	153.98	131.48	23.69	28.13	81.42	208.12	313.65	429.27	399.78	475.12	500.62
2906	0.75	18.83	41.81	52.99	88.64	78.29	39.08	70.27	126.08	149.83	178.07	230.27	193.56	249.65	251.26	231.53
2912	13.52	23.56	53.57	90.37	64.36	32.05	26.7	87.73	99.86	136.07	184.46	152.54	190.56	226.19	190.70	
2918	25.65	58.36	89.92	87.9	34.76	46.47	37.3	34.75	20.62	62.1	60.84	66.37	101.92	96.65		
3000	43.27	84.84	85.12	28.48	56.86	31.48	49.05	81.07	133.95	134.3	97.39	48.59	21.37			
3006	38.32	72.65	44.52	39.57	28.9	35.3	59.7	67.12	18.67	85.36	156.8	91.67				
3012	26.15	21.52	30.78	63.57	147.83	192.9	205.29	142.96	111.33	112.94	52.42					
3018	43.72	33.41	32.89	9.88	29.57	33.73	59.66	83.02	113.18	60.79						
0100	16.71	43.29	34.54	52.62	76.2	46.7	2.36	2.03	29.94							
0106	42.88	47.38	19.95	45.29	41.75	32.23	57.03	131.83								
0112	27.02	3.23	12.13	18.67	13.37	56.05	6.61									
0118	5.04	3.71	10.49	86.73	64.1	135.20										
0200	29.49	22.09	17.81	36.58	91.59											
0206	7.29	5.6	5.61	42.44												
0212	8.7	7.04	53.39													
0218	14.91	33.41														
Mean Error	27.83	41.31	48.12	56.82	64.25	73.94	71.4	81.55	76.04	101.42	116.22	129.38	157.47	187.52	246.81	308.69

Table 4: Along track error of SAC-Lagrangian advection track prediction model for TC FANI w.r.t JTWC real-time observed track

FCST Initial time	Track Error (km) in different Forecast Lead time															
	6	12	18	24	30	36	42	48	54	60	66	72	78	84	90	96
2700	2.17	11.88	48.99	125.64	137.19	0	224.45	237.17	280.93	186.83	174.46	106.07	139.98	128.09	67.51	39.88
2706	0.12	10.62	46.01	11.43	0	46.77	55.77	77.08	11.89	48.15	107.41	111.88	120.94	173.78	153.77	0
2712	10.34	14.66	40.18	0	24.18	15.18	76.37	102.42	120.8	118.71	123.27	123.93	153.26	167	0	30.92
2718	17.24	16.4	0	5.98	38.67	77.84	61.32	71.41	61.12	97.15	87.62	112.83	98.83	0	89.44	0
2800	52.8	0	63.78	35.85	20.83	56.37	49.88	61.59	50.96	46.48	41.72	12.13	0	165.99	0	21.58
2806	0	21.36	14.97	23.15	36.18	23.01	4.92	7.48	17.17	52.25	75.51	0	90.23	0	168.68	61.47
2812	12.9	44.45	94.61	129.09	147.89	159.73	162.84	158.96	189.69	166.64	0	109.72	0	68.58	148.27	304.77
2818	8	20.23	64.34	107.5	139.73	182.2	193.43	224.94	202.1	0	84.01	0	103.07	208.49	353.34	67.41
2900	13.19	1.07	33.71	67.46	71.25	69.73	106.63	115.05	0	85.12	0	18.48	73.29	218.03	7.35	137.78
2906	17.31	6.86	4.57	8.21	0.49	19.16	0.99	0	28.98	0	22.54	57.74	133.46	22.7	10.6	66.53
2912	12.08	10.2	11.33	11.17	33.57	25.25	0	18.8	0	2.06	41.76	119.77	55.44	18.08	30.76	
2918	14.41	25.99	32.43	26.2	64.69	0	48.44	0	2.41	38.77	64.94	38.32	10.86	18.96		
3000	4.15	3.9	24.53	52.14	0	27.46	0	37.42	40.95	38.39	38.32	18.59	3.74			
3006	8.25	22.11	18.1	0	9.74	0	59.2	133.9	159.38	162.36	157.25	158.31				
3012	13.17	8.81	0	76.47	0	15.21	48.71	91.33	36.65	78.49	114.51					
3018	11.3	0	26.97	0	5.61	64.08	81.94	61.92	74.74	99.87						
0100	0	13.91	0	39.25	10.18	0	26.61	91.8	90.86							
0106	1.73	0	23.07	25.63	43.18	25.45	40.89	22.65								
0112	0	49.99	70.11	54.83	70.2	97.62	108.52									
0118	16.63	17.86	5.61	0	104.89	91.83										
0200	16.85	9.71	1.05	43.73	36.64											
0206	17.39	4.2	28.96	0.81												
0212	8.71	19.21	15.64													
0218	3.44	3.77														
Mean Error	10.92	14.05	29.09	38.39	47.39	49.84	71.1	84.11	80.51	76.33	75.55	70.56	75.62	99.14	93.61	73.04

Table 5: Direct position error of SAC-Lagrangian advection track prediction model for TC FANI w.r.t IMD Best Track

FCST Initial time	Track Error (km) in different Forecast Lead time															
	6	12	18	24	30	36	42	48	54	60	66	72	78	84	90	96
2700	62.01	111.45	159.78	210.91	210.68	246.63	278.94	302.46	318.84	296.49	254.03	206.97	161.65	128.09	67.75	44.93
2706	35.42	56.95	69.59	73.44	136.20	154.58	170.56	158.08	144.66	131.59	124.70	121.47	126.01	173.80	217.46	247.53
2712	43.03	47.19	46.45	121.55	95.30	65.42	76.40	103.55	121.71	121.48	163.80	222.61	219.11	167.86	73.64	42.87
2718	39.63	26.16	69.11	63.89	66.05	80.46	76.47	76.30	61.55	129.08	174.61	162.21	99.17	33.66	96.68	169.36
2800	53.81	83.02	84.95	53.21	32.29	56.68	52.58	63.35	79.07	108.28	75.75	18.95	87.94	226.84	315.79	412.45
2806	50.17	62.26	54.26	23.45	36.81	23.02	12.28	52.68	61.31	87.43	122.43	173.17	289.79	355.84	402.50	438.14
2812	16.38	45.72	103.12	130.96	149.01	160.58	185.64	232.83	226.71	169.10	102.55	109.94	190.65	324.55	458.34	547.36
2818	35.67	66.54	81.69	112.11	141.35	209.40	271.51	264.18	208.26	139.74	91.47	187.07	294.03	447.78	543.57	591.00
2900	46.09	64.99	84.95	97.88	121.52	169.03	169.29	117.47	28.13	117.79	208.12	314.20	435.48	455.36	475.17	519.24
2906	17.33	20.04	42.05	53.62	88.64	80.60	39.10	70.27	129.37	149.83	179.49	237.40	235.11	250.68	251.48	240.90
2912	18.13	25.67	54.75	91.06	72.58	40.80	26.70	89.72	99.86	136.08	189.13	193.94	198.46	226.91	193.16	
2918	29.42	63.88	95.59	91.72	73.44	46.47	61.14	34.75	20.76	73.21	88.99	76.64	102.50	98.49		
3000	43.47	84.93	88.59	59.41	56.86	41.77	49.05	89.29	140.06	139.68	104.66	52.02	21.69			
3006	39.20	75.94	48.06	39.57	30.50	35.30	84.07	149.78	160.47	183.44	222.07	182.94				
3012	29.28	23.25	30.78	99.44	147.83	193.49	210.99	169.65	117.21	137.54	125.94					
3018	45.15	33.41	42.53	9.88	30.10	72.42	101.36	103.57	135.62	116.92						
0100	16.71	45.47	34.54	65.64	76.87	46.70	26.71	91.82	95.66							
0106	42.92	47.38	30.50	52.04	60.07	41.07	70.18	133.76								
0112	27.02	50.09	71.15	57.92	71.46	112.57	108.72									
0118	17.38	18.24	11.90	86.73	122.93	163.43										
0200	33.97	24.13	17.84	57.02	98.65											
0206	18.86	7.00	29.50	42.45												
0212	12.31	20.46	55.64													
0218	15.31	33.62														
Mean Error	32.86	47.41	61.19	77	91.39	102.02	109.04	127.97	126.43	139.86	148.52	161.39	189.35	240.82	281.41	325.38

IMD reported that cyclone crossed Odhisa coast near Puri at latitude 19.8 and longitude 85.7 (9:30 AM IST) between 0800-1000 IST of 3rd MAY, 2019. The landfall point and time error of all the real-time generate track forecasts by SAC-model has been computed with respect to IMD estimated landfall position and have been summarized in the Table 6.

Table 6: Land-fall point error (km) of SAC-Lagrangian advection track prediction model for TC FANI

Forecast initial time	Landfall point		Landfall time (after FCST initial time)	Landfall Error	
	Longitude	Latitude	Lead Hours	Position Error (km)	Time Error (hours)
2906	84.71	19	102 (3 May 12 Z)	136.73	+8
2912	85.15	19.44	95 (3 May 11 Z)	70.15	+7
2918	85.57	19.69	88 (3 May 12 Z)	18.29	+8
3000	85.72	19.76	77 (3 May 05 Z)	4.92	+1
3006	83.3	17.69	58 (2 May 16 Z)	344.82	-12
3012	84.32	18.52	60 (3 May 00 Z)	203.14	-4
3018	84.38	18.6	55 (3 May 01 Z)	192.4	-3
0100	84.76	19.07	46 (3 May 12 Z)	127.69	+8
0106	85.46	19.64	42 (3 May 00 Z)	30.78	-4
0112	84.37	18.59	32 (2 May 20 Z)	193.93	-8
0118	85	19.32	26 (2 May 20 Z)	90.71	-8
0200	85.36	19.59	24 (3 May 00 Z)	42.57	-4
0206	85.54	19.67	21 (3 May 03 Z)	22.12	-1
0212	85.49	19.65	15 (3 May 03 Z)	27.59	-1
0218	85.63	19.72	10 (3 May 04 Z)	11.52	0

It can be seen that landfall error, of track predicted before 24 hours (00 UTC 02 MAY 2019), in position was 42 km and time was four hours advance.

The forecasts from SAC model can be further improved by including the high resolution (17 km x 17 km) first guess conditions provided by NCMUM model from National Centre of Medium Range Weather Forecast (NCMRWF) in place of currently being used 50 km x 50 km gfs initial conditions.

3.3 Intensity Prediction of TC FANI

Intensity of TC FANI was predicted using output of HWRf model which is operationally run at NCEP. Real-time generated intensity product is shown in the figure.

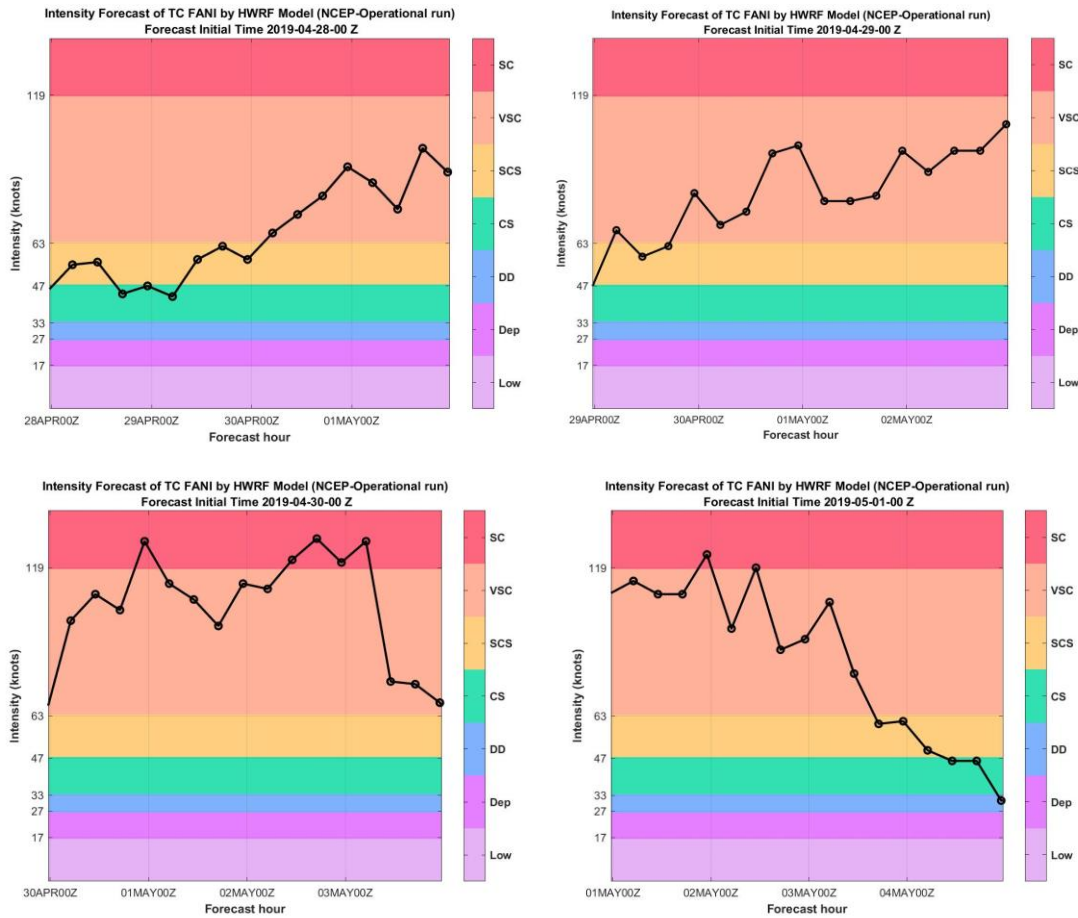


Figure 6: Real-time generated intensity prediction of TC FANI during 00 UTC of 28 April- 01 May, 2019.

3.4 Ship Avoidance Region Prediction for TC FANI

For vessels at sea, avoiding the 34 knot wind field of a tropical cyclone is paramount. Any ship in the vicinity of a tropical cyclone should make every effort to remain clear of the maximum radius of analyzed or forecast 34 knot winds associated with the tropical cyclone. Knowing that the area of 34 knot around tropical cyclones is rarely symmetric but instead varies within semi-circles or quadrants is important. Understanding that each tropical storm or hurricane has its own unique 34 knot wind field are necessary factors to account for when attempting to remain clear of this dangerous area around a tropical cyclone. Based on operational HWRP 34 knot wind radial distances the graphical inputs of ship avoidance region was also generated for TC FANI and disseminated through SCORPIO server.

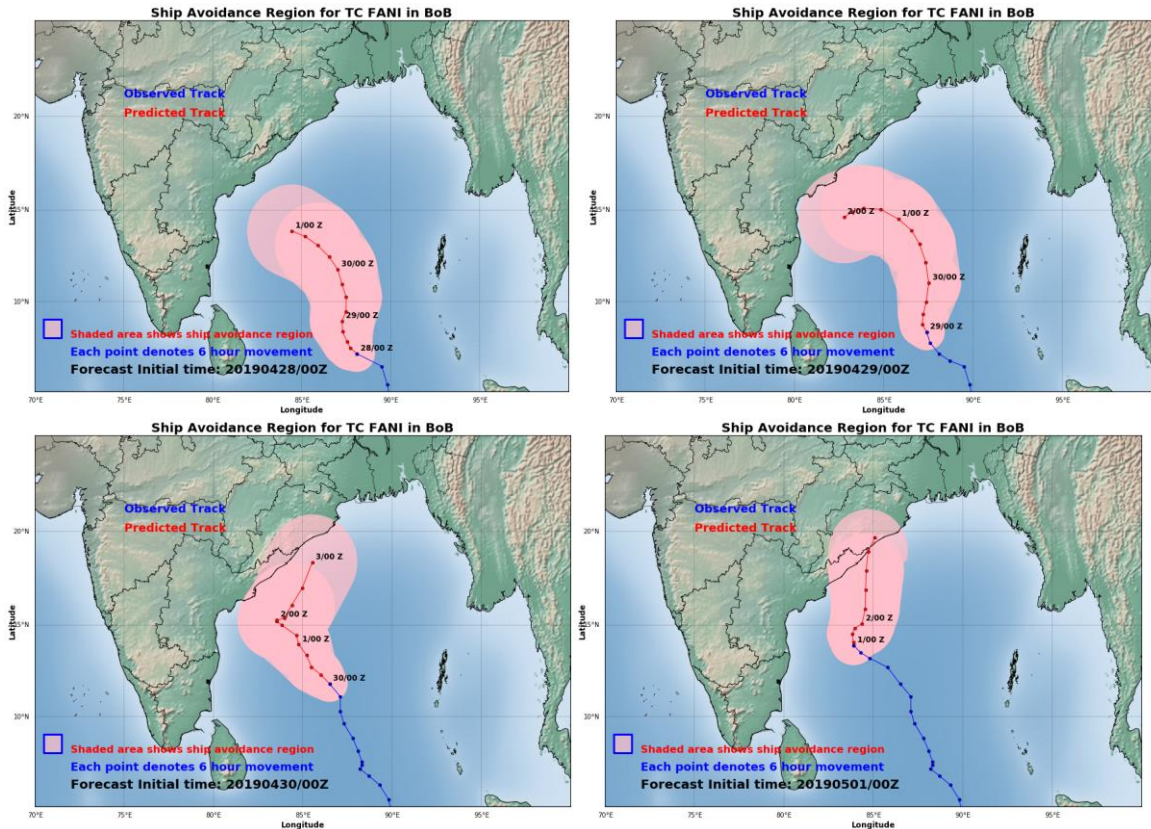


Figure 7: Real-time predicted ship avoidance region for TC FANI during 00 UTC of 28 April- 01 May, 2019.

4. Satellite Observations over TC FANI

Different sensors onboard the geostationary and polar orbiting satellites provide observations at different times and different phases of intensification of TCs which are very useful to estimate the correct geo-location of the system and retrieve its structural parameters. Different satellite observations over TC FANI have been discussed in this section.

4.1 INSAT 3D

Cyclone Geo-location

TC FANI was continuously observed by the half hourly acquisition of INSAT-3D satellite. In half hourly TIR imageries of INSAT 3D satellite the center location of cyclone was estimated by center determination algorithm developed at SAC. The results were disseminated through SCORPIO web-server. One of the sample products generated in the real-time has been shown in the Fig. 8.

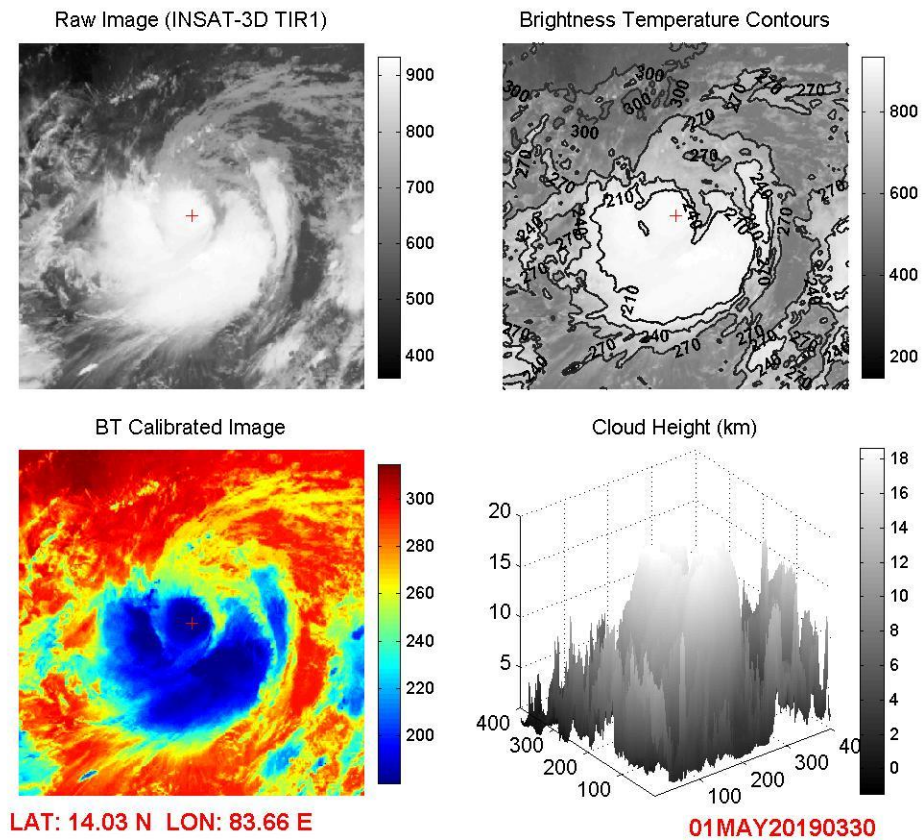


Figure 8: Center of TC estimated using INSAT 3D TIR image (0030Z 01 May, 2019).

Cyclone centric products of INSAT3D satellite

A procedure has been developed to produce cyclone centric products from each half hourly image of INSAT3D satellite. These images are very useful to study the structural changes in the core of tropical cyclone. A sample product generated on 0330 Z 30 April, 2019 have been presented in the Figure 9.

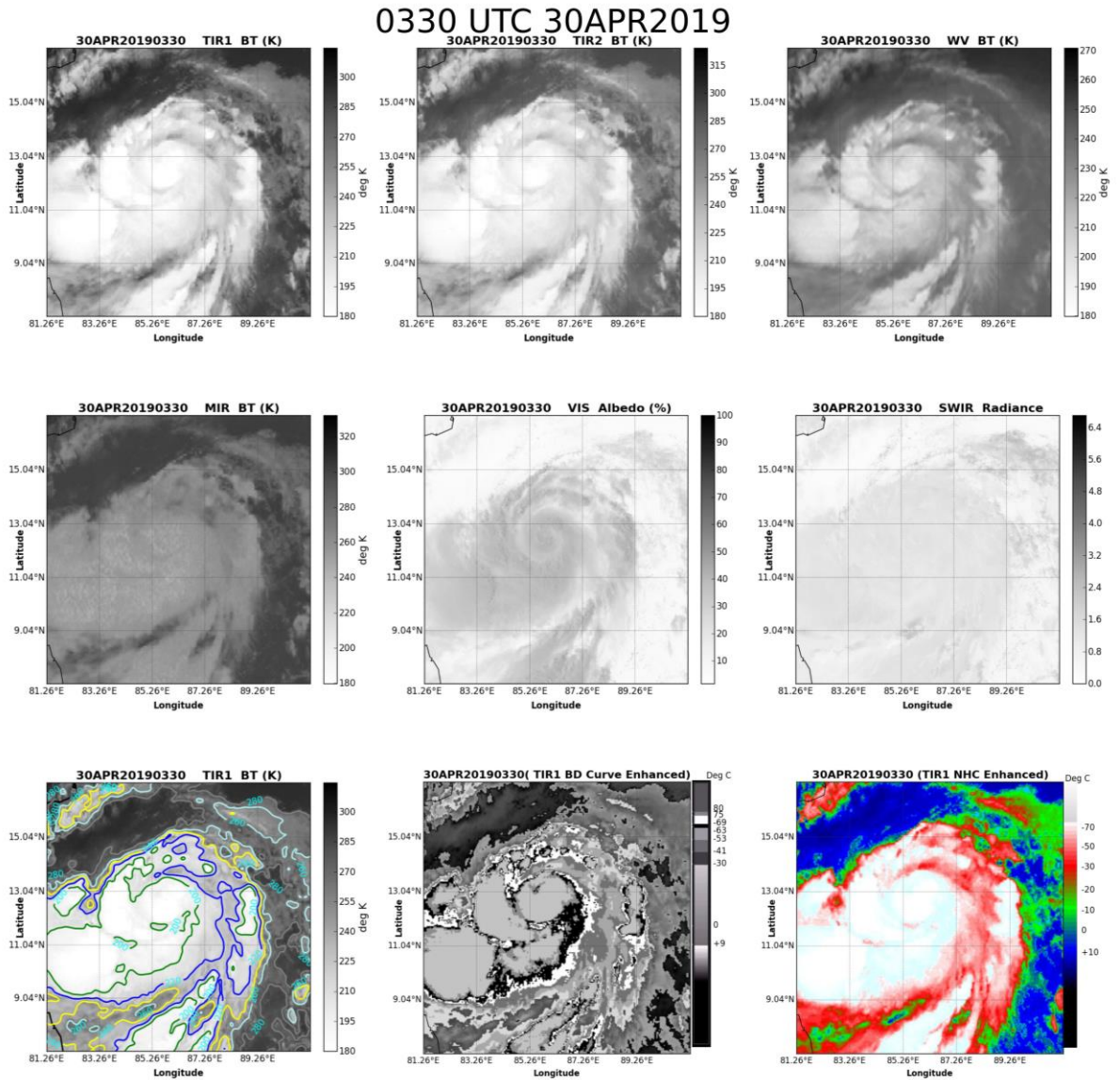


Figure 9: Cyclone centric products of INSAT3D imager channels

4.2 SAPHIR

SAPHIR onboard Megha-Tropiques satellite is a sounding instrument with six channels near the absorption band of water vapor at 183.31 GHz. The channels provide continuous observations of 10 km resolution (at nadir) at 6 different atmospheric layers at least 2-3 times in a day. These high resolution data was found very useful to observe the internal changes in the cyclone structure during the intensification process of TCs. SAPHIR onboard Megha-Tropiques satellite is a sounding instrument with six channels near the absorption band of water vapor at 183.31 GHz. The channels provide continuous observations of 10 km resolution (at nadir) at 6 different atmospheric layers. The BT values observed from SAPHIR over TC FANI have been shown in the Fig. 10. The lower level structure of cyclone during 1st and 2nd May shows very clearly its inner core spiral bands with its well-formed eye. On 2nd May observation the very high BT values were found in the eye.

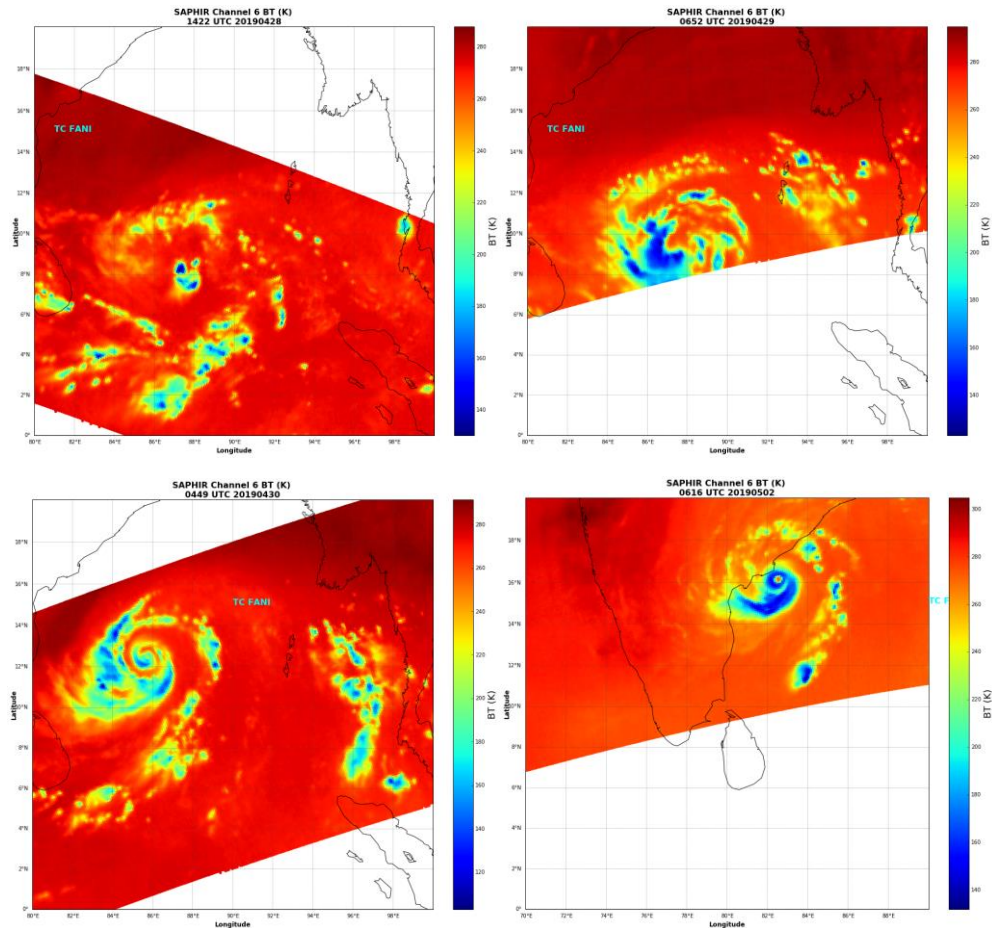


Figure 10: BT values observed by SAPHIR channel-6 over the tropical cyclone FANI

4.3 Satellite based surface wind observations over TC FANI

The wind observations over TC FANI observed by different sensors onboard different Indian and foreign satellites e.g. SCTASAT-1, CYGNSS, SMAP and WINDSAT have been discussed in this section.

4.3.1 SCATSAT-1

The SCATSAT-1 satellite had six coverage over cyclone FANI during its life over ocean. The wind vectors (L2B: 25 km x 25 km) from all the pass covering the cyclonic have been shown in the Figure 11. The observations of surface wind vectors over TC FANI by SCATSAT-1 have been analyzed. The maximum wind speed captured by the SCATSAT passes have been shown in the Figure 16 along with JTWC maximum sustained wind speed. The JTWC wind speed are converted into 10 minute averaged wind by multiplying the factor 0.9. The satellite estimates are equivalent to 10 minute average wind speed values. The four SCATSAT passes shows the full coverage over the system however, the pass on 30 April (morning) is showing the partial coverage and 2nd May (evening) shows the system close to land.

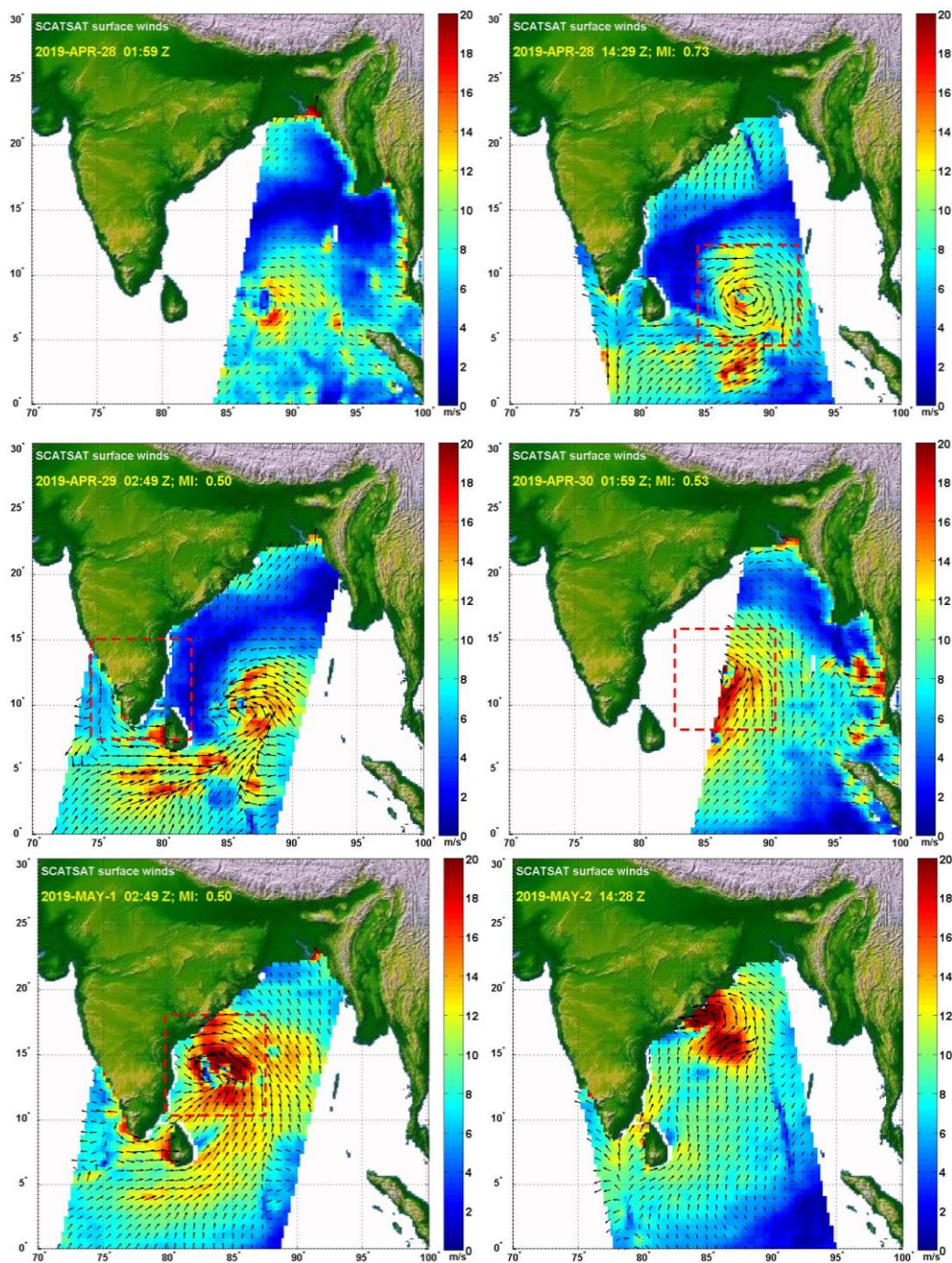


Figure 11: SCATSAT-1 wind vector products over the TC FANI (28th April -02nd May, 2019)

4.3.2 CYGNSS

CYGNSS (Cyclone Global Navigation Satellite System) is part of the NASA ESSP (Earth System Science Pathfinder) program referred to as an EVM (Earth Venture Mission). CYGNSS will use a constellation of eight small satellites in LEO (Low Earth Orbit) carried to orbit on a single launch vehicle. In orbit, CYGNSS's eight microsatellite observatories will receive both direct and reflected signals from GPS (Global Positioning System) satellites. The direct signals pinpoint CYGNSS observatory positions, while the reflected signals respond to ocean surface roughness, from which wind speed is retrieved.

The overall objective of CYGNSS is to improve extreme weather predictions. The mission is focused on tropical cyclone (TC) inner core process studies. CYGNSS attempts to resolve the principle deficiencies with current TC intensity forecasts, which lie in inadequate observations and modeling of the inner core. The inadequacy in observations results from two causes viz. (i) much of the inner core ocean surface is obscured from conventional remote sensing instruments by intense precipitation in the eye wall and inner rain bands and (ii) the rapidly evolving (genesis and intensification) stages of the TC life cycle are poorly sampled in time by conventional polar-orbiting, wide-swath surface wind imagers. CYGNSS is specifically designed to address these two limitations by combining the all-weather performance of GNSS bistatic ocean surface scatterometry with the sampling properties of a constellation of eight satellites. The use of a dense constellation of microsatellites results in spatial and temporal sampling properties that are markedly different from conventional imagers.

The observations by the constellations of CYGNSS system over TC FANI have been shown in the Figure 12. All the passes within a day have been plotted together. The maximum wind speed observed by the satellite system has been summarized in the Fig. 16.

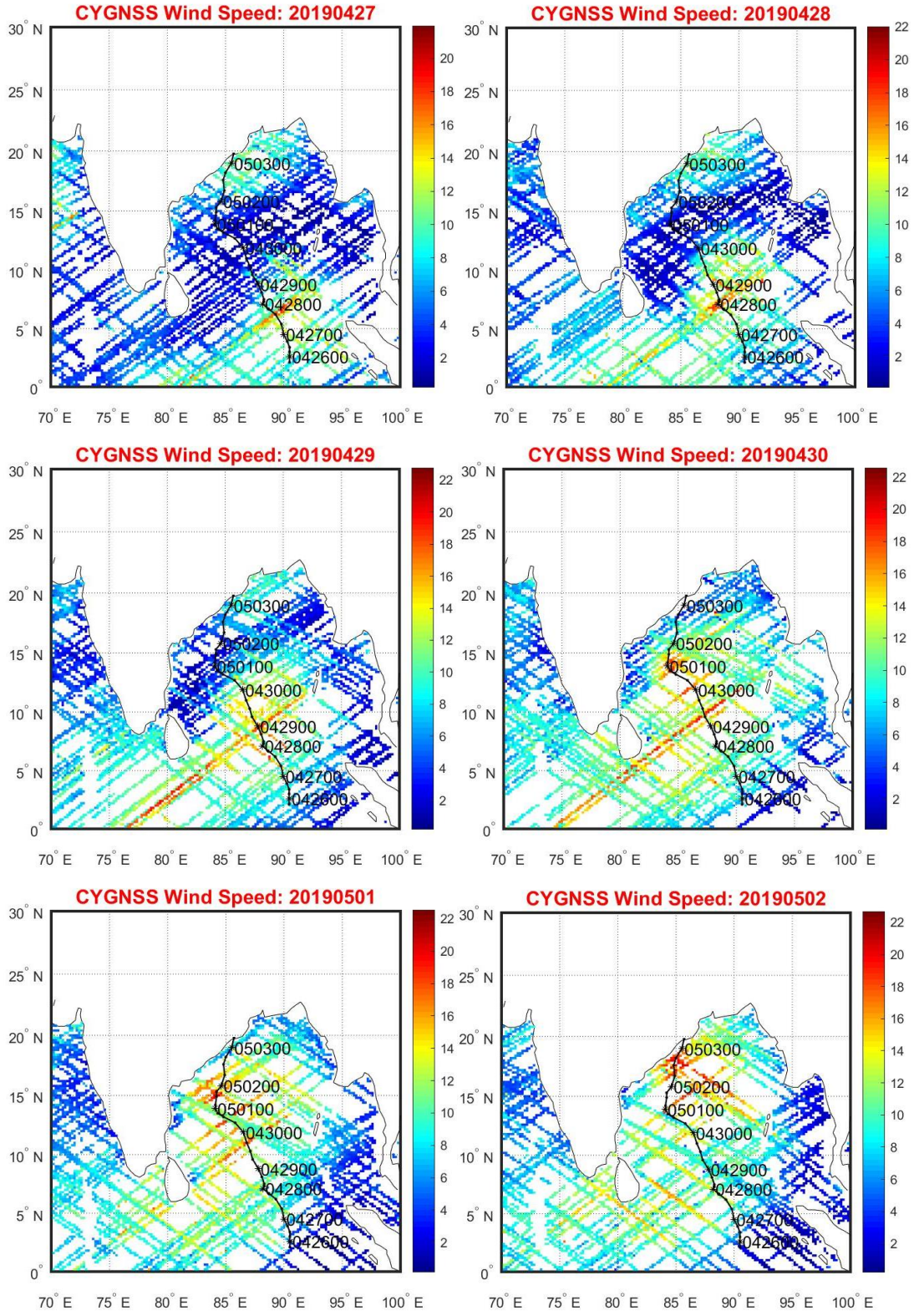


Figure 12: GYGNSS wind speed products over the TC FANI (27th April -02nd May, 2019)

4.3.3 SMAP

Soil Moisture Active Passive (SMAP) is a United States environmental research satellite launched on 31 January 2015. The SMAP observatory includes a dedicated spacecraft and instrument suite in a near-polar, Sun-synchronous orbit. The SMAP measurement system consists of a radiometer (passive) instrument and a synthetic aperture radar (active) instrument operating with multiple polarizations in the L-band range. The combined active and passive measurement approach takes advantage of the spatial resolution of the radar and the sensing accuracy of the radiometer.

SMAP provides two wind speed products e.g. (i) Near-Real Time (NRT) wind speed and (ii) Final wind speed product. The NRT wind processing uses ancillary fields of shorter latency but lower quality. A Final Wind Speed version, reprocessed with a 1-month delay, which uses higher quality ancillary data. The wind speed from NRT product of SMAP over TC FANI has been shown in the Fig. 13. There were five passes of SMAP over the TC FANI during its different intensity stages.

Additionally, SMAP also provide Tropical Cyclones (TC) ASCII files with SMAP 10-min maximum-sustained winds (in kn) and wind radii (in nm) for the 34 kn (17 m/s), 50 kn (25 m/s), and 64 kn (33 m/s) winds for each SMAP pass over a TC in all tropical ocean basins. The wind radii estimated by SMAP satellite for TC FANI for four of its full coverage pass has been shown in the Figure 14. The values have been summarized in Table 7.

Table 7: Critical wind radii estimates by SMAP product

Pass Time (MMDD)	Maximum Wind (kt)	R34: 34 knots wind radii (nm)				R50: 50 knots wind radii (nm)				R64: 64 knots wind radii (nm)			
0428	42	0	0	58	0	0	0	0	0	0	0	0	0
0430	87	83	108	95	89	39	66	66	57	29	40	39	31
0501	96	80	132	117	85	53	70	66	43	40	52	39	31
0502	148	0	154	0	0	0	68	0	0	0	50	0	0

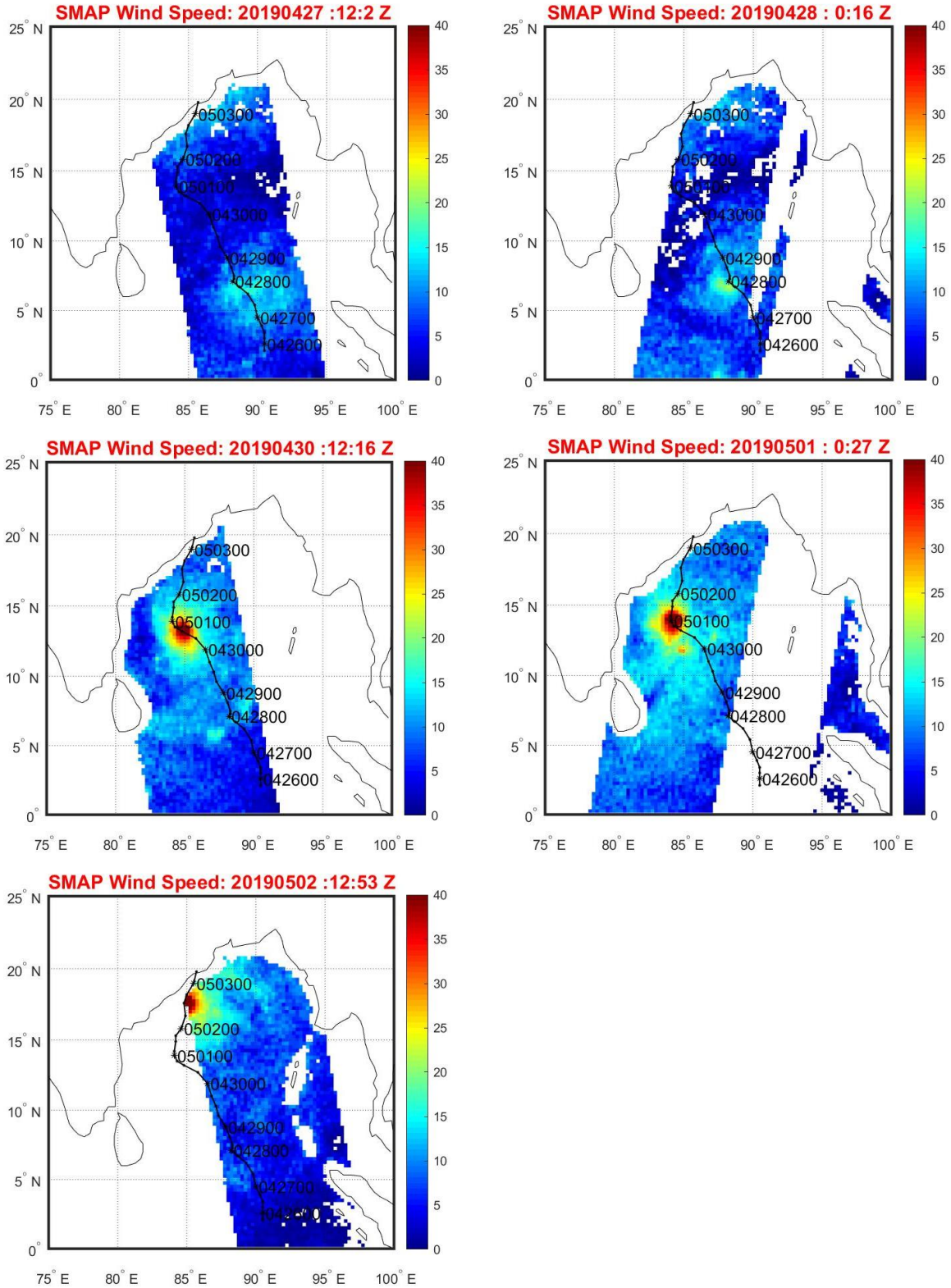


Figure 13: SMAP wind speed NRT products over TC FANI (27th April -2nd May 2019)

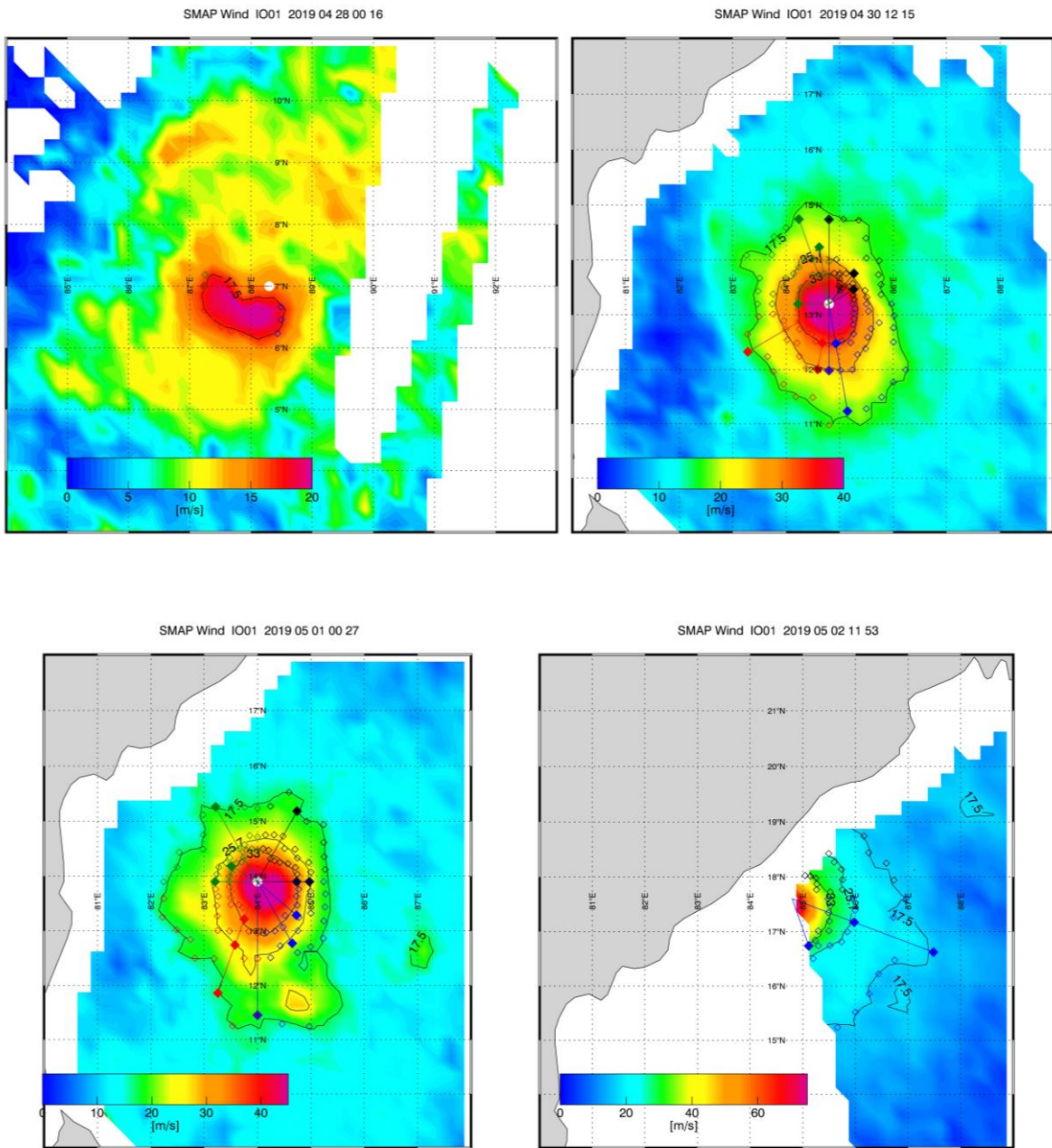


Figure 14: SMAP critical wind radii estimation over TC FANI

4.3.4 WINDSAT

The WindSat Polarimetric Radiometer was developed by the Naval Research Laboratory (NRL) Remote Sensing Division and the Naval Center for Space Technology for the U.S. Navy and the National Polar-orbiting Operational Environmental Satellite System (NPOESS) Integrated Program Office (IPO). It was launched on January 6, 2003 aboard the Department of Defense Coriolis satellite. WindSat was meant to demonstrate the capabilities of a fully polarimetric radiometer to measure the ocean surface wind vector from space. Prior to launch, the only instrument capable of measuring ocean wind vectors were scatterometers (active microwave sensors). In addition to wind speed and direction, the instrument can also measure sea surface temperature, soil moisture, ice and snow characteristics, water vapor, cloud liquid water, and rain rate.

The near real time (NRT) product of all-weather wind speed, WSPD_AW, over TC FANI have been shown in the Figure 15. The final WSPD_AW product is generated after a month which is a smooth blend between the standard wind speed obtained in non-raining conditions WSPD_LF, the global wind speed through rain and the H-wind derived wind speed.

There were two full and two partial coverage of WINDSAT over TC FANI. The maximum wind speed observed by NRT product in all these passes were analysed and summarized in Figure 16.

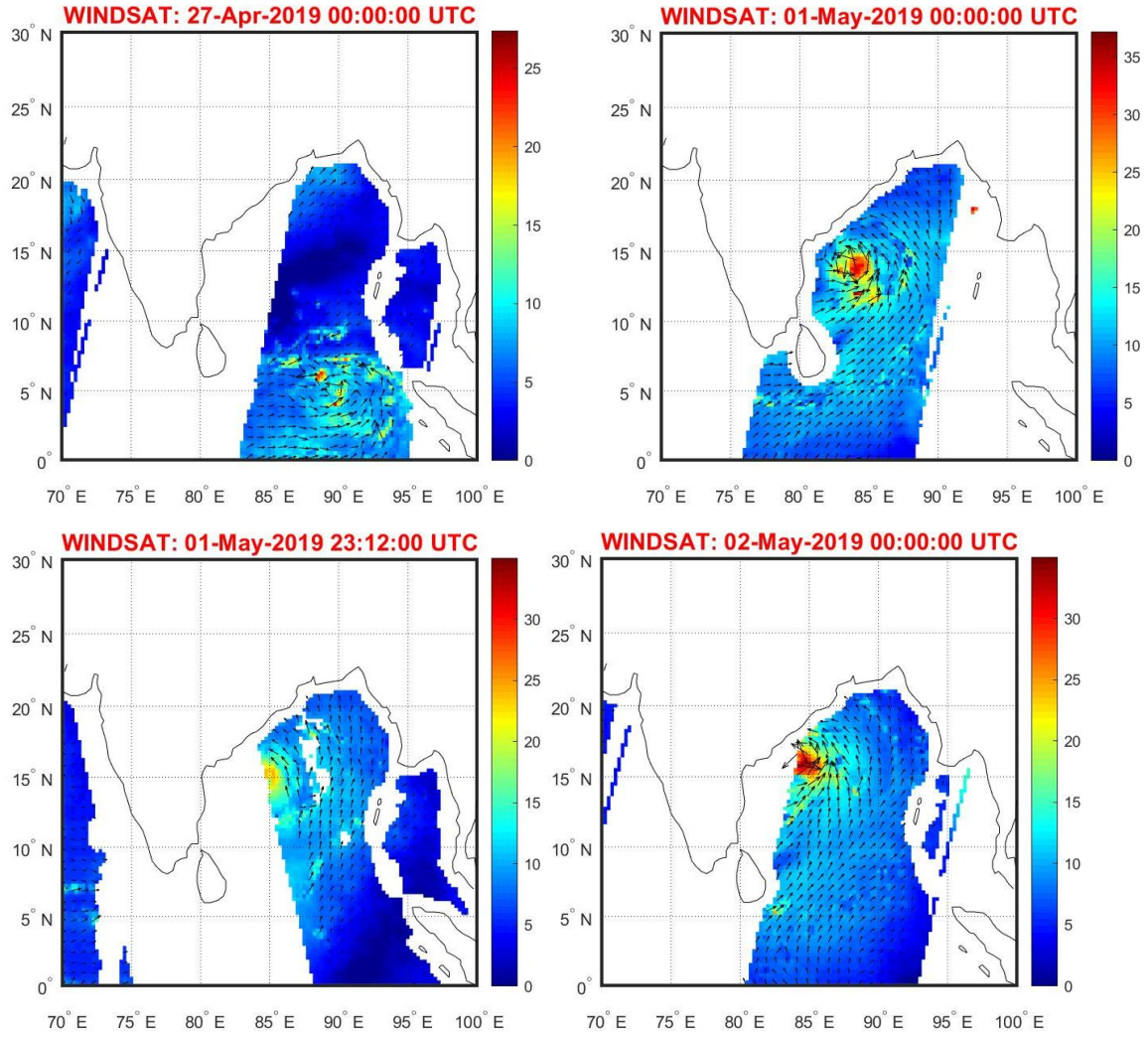


Figure 15: WINDSAT wind vectors NRT products over TC FANI (27th April -2nd May 2019)

4.3.5 Comparison of Satellite Wind Speed Products

The maximum wind speed estimated in the inner core of the cyclone during its pass over TC FANI by all the above mentioned satellites have been shown in the Figure 16. The JTWC real-time estimated wind speed at every 6-hour interval is also plotted in the figure. The figure shows that SCATSAT-1 gives good estimates of wind speed upto 30 m/s. After that the values are underestimated. This underestimation by SCATSAT for higher winds is due to its obvious reason of backscatter signal contamination during high rain conditions. The values of SMAP were found to be very well estimated with the JTWC observed wind estimates. SMAP has found to be accurately estimating the winds upto nearly 50 m/s. The maximum wind speed estimated by CYGNSS wind product was upto approximately 21 m/s only. The high winds are not found to be captured by CYGNSS wind product. WINDSAT wind speed estimates were also underestimated during very high wind speed conditions i.e. beyond 40 m/s. TC FANI was extremely severe cyclone with wind speed upto 60 m/s. The SMAP satellite wind products have shown their potential to estimate such high wind estimates. The analysis is based on the NRT products which shows that SMAP wind can also be utilized during real-time.

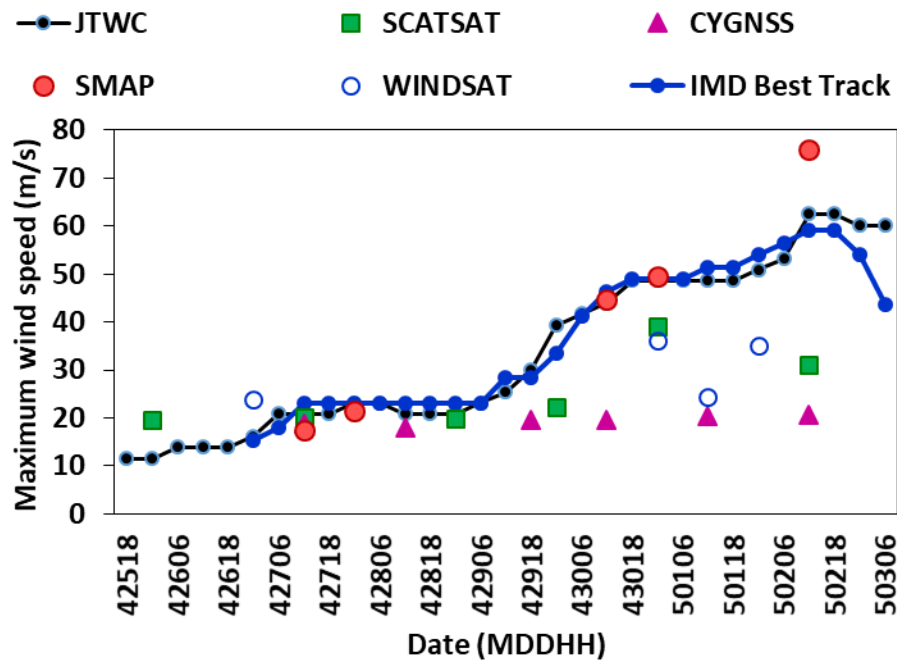


Figure 16: Inter-comparison of maximum wind speed estimated by satellite products over TC FANI

5. Conclusions

The real-time monitoring and prediction of TC FANI based on in-house developed techniques and the satellite products have been summarized in this report.

The real-time track prediction of track TC based on in-house developed model SAC-LAGAM for different initial conditions at 00 06 12 and 18 UTC during 27 April to 02 May 2019 have been presented in the report. The track error with respect to JTWC observed track has been computed for all forecast lead hours. It has been shown that for TC FANI the mean track error (direct position error) for lead prediction time 24, 48, 72 and 96 hours was 77 km, 128 km, 161 km and 325 km, respectively. The landfall position and time accuracy for 24 hour lead time (FCST initial time: 02 May 00Z) was 43 km with 4 hours early. For 10 hour lead time (FCST initial time: 02 May 18Z) the location error was 12 km with accurate landfall time.

Scatsat-1 did not capture the cyclone during its genesis stage. The cyclogenesis of TC FANI observed by NCEP-GFS model using genesis potential parameter has been discussed. It has been found that based on GPP, TC FANI was predicted as a developing system on 00 UTC 23 April 2019 as the GPP values at the vortex were exceeding the predetermined threshold.

The real-time satellite cyclone centric products on Indian satellite INSAT-3D, SCATSAT-1 and SAPHIR has also been discussed in this report. During the life time of TC FANI, there were five passes of SCATSAT with full coverage over the system. Each day at least one full coverage pass of SAPHIR was available over the system. In the advance stage of the system SAPHIR was showing a very clear eye and eyewall structure distinguished by sharp BT gradients.

The real-time products of TC intensity forecast and ship avoidance region prediction based on the NCEP-operational hurricane-WRF model has been presented in this report.

The wind speed estimated by different satellite products (available in near real-time) have been presented in this report for all passes of satellites (SCATSAT-1, CYGNSS, SMAP and WINDSAT). It has been shown that the high winds over the extremely severe TC FANI was very well estimated by SMAP wind products. In addition to wind speed, the

SMAP estimated critical wind radii estimates (R34, R50 and R64) for all its passes over TC FANI have been also presented. These products are very useful for assessing the cyclone related damage assessment during its landfall.

The future scope of the works include the analysis of satellite estimates using the final products which is generated after 1-2 month delayed mode.

References

1. Brand, S., Buenafe, C. A. and Hamilton, H. D. (1981). Comparison of tropical cyclone motion and environmental steering. *Mon Wea Rev* 108:908-909.
2. Chan, J.C.L. and Williams, R.T. (1987). Analytical and numerical studies of the beta-effect in tropical motion. *J Atmos Sci* 44:1257-1265.
3. Frank, Neil L., Husain, S. A., 1971. The Deadliest Tropical Cyclone in History. *Bull. Amer. Meteor. Soc.*, 52, 438–445.
4. Heming J. T. (1994). Keeping an eye on the hurricane -Verification of tropical cyclone forecast tracks at the UK Meteorological Office. *NWP Gazette*,1, No.2, pp.3 -8.
5. Hoover, B.T. and Morgan M.C. (2006). Effects of cumulus parameterization on tropical cyclone potential vorticity structure and steering flow. Preprints of the 27th AMS Conference on Hurricanes and Tropical Meteorology. April 23-28 Monterey, CA, paper 8B.5.
6. IMD Report, (2015a). Cyclonic Storm, ASHOBAA over the Arabian Sea (07-12 June 2015): A Report. Cyclone Warning Division, India Meteorological Department, New Delhi. June 2015.
7. IMD Report, (2015b). Extremely Severe Cyclonic Storm, CHAPALA over the Arabian Sea (28 October - 4 November, 2015): A Report. Cyclone Warning Division, India Meteorological Department, New Delhi. December 2015.
8. IMD Report, (2015c). Extremely Severe Cyclonic Storm, MEGH over the Arabian Sea (05 - 10 November, 2015): A Report. Cyclone Warning Division, India Meteorological Department, New Delhi. December 2015.
9. IMD Report, (2018). Cyclonic Storm “Daye” over eastcentral Bay of Bengal and adjoining Myanmar (19-22 September 2018): Summary. Regional Specialised Meteorological Centre-Tropical Cyclones, New Delhi, India Meteorological Department, New Delhi. October 2018.
10. IMD Report, (2018). Very Severe Cyclonic Storm “Titli” over eastcentral Bay of Bengal (08-13 October 2018): Summary. Regional Specialised Meteorological Centre-Tropical Cyclones, New Delhi, India Meteorological Department, New Delhi. October 2018.
11. Jaiswal, N., Kishtawal, C. M., Bhomia, S. and Pal, P. K. (2016). Multi-model ensemble based probabilistic prediction of tropical cyclogenesis using TIGGE Model Forecasts. *Meteorology and Atmospheric Physics*. DOI 10.1007/s00703-016-0436-2.

12. Jaiswal, N., and Kishtawal, C. M., (2011a). Prediction of Tropical Cyclogenesis Using Scatterometer Data. *IEEE Transaction on Geoscience and Remote Sensing*, vol. 49, Issue 12, pp. 4904 – 4909.
13. Jaiswal, N., and Kishtawal, C. M., (2011b). Automatic Determination of Center of Tropical Cyclone in Satellite-Generated IR Images. *IEEE Geoscience and Remote Sensing Letters*. vol. 8, No. 3, pp. 460-463.
14. Jaiswal, N., and Kishtawal, C. M., (2012). Objective Detection of Center of Tropical Cyclone in Remotely Sensed Infrared Images. *IEEE Journal of Selected Topics in Applied Earth Observations and Remote Sensing*. DOI.10.1109/JSTARS.2012.2215016.
15. Jaiswal, N., Kishtawal, C. M., and Pal, P. K., (2013). Prediction of Tropical Cyclogenesis in North Indian Ocean using OSCAT Data. *Meteorology Atmospheric Physics*, vol. 119, pp. 137–149.
16. Kotal S., Kundu P. and Bhomick, S. K. (2009). Analysis of cyclogenesis parameter for developing and nondeveloping low-pressure systems over the Indian Sea.
17. Kotal S., and Bhattacharya, (2013). Tropical cyclone Genesis Potential Parameter (GPP) and it's application over the north Indian Sea. *Mausam* 64(1):149-170.
18. Singh, Sanjeev Kumar, Kishtawal, C.M, and Pal, P. K. (2012a). Track prediction of Indian Ocean cyclones using Lagrangian advection model. *Nat. Hazards*, Vol.63, no.3, 62:745-778.
19. Singh, S. K., Kishtawal, C. M., Jaiswal, N., Singh, R. and P. K. Pal, (2012b). Impact of Vortex-Removal from Environmental Flow in Cyclone Track Prediction using Lagrangian Advection Model. *Meteorology Atmospheric Physics*, vol. 117, pp. 103–120.